

# Waste Package Performance Assessment:

## Deterministic System Model Program Scope and Specification

W. J. O'Connell

R. S. Drach

October 1986



Lawrence  
Livermore  
National  
Laboratory

9003010466 900221  
PDR WASTE PDC  
WM-11

ENCLOSURE 2 102

**DISCLAIMER**

This document was prepared as an account of work sponsored by an agency of the United States Government. Neither the United States Government nor the University of California nor any of their employees, makes any warranty, express or implied, or assumes any legal liability or responsibility for the accuracy, completeness, or usefulness of any information, apparatus, product, or process disclosed, or represents that its use would not infringe privately owned rights. Reference herein to any specific commercial products, process, or service by trade name, trademark, manufacturer, or otherwise, does not necessarily constitute or imply its endorsement, recommendation, or favoring by the United States Government or the University of California. The views and opinions of authors expressed herein do not necessarily state or reflect those of the United States Government or the University of California, and shall not be used for advertising or product endorsement purposes.

Prepared by Nevada Nuclear Waste Storage Investigation (NNWSI) Project participants as part of the Civilian Radioactive Waste Management Program. The NNWSI Project is managed by the Waste Management Project Office of the U.S. Department of Energy, Nevada Operations Office. NNWSI Project work is sponsored by the Office of Geologic Repositories of the DOE Office of Civilian Radioactive Waste Management.

Work performed under the auspices of the U.S. Department of Energy by the Lawrence Livermore National Laboratory under Contract W-7405-Eng-48.

# Waste Package Performance Assessment:

## Deterministic System Model Program Scope and Specification

W. J. O'Connell

R. S. Drach

Manuscript date: October 2, 1986

**LAWRENCE LIVERMORE NATIONAL LABORATORY**  
University of California • Livermore, California • 94550



# Contents

List of Figures .....	iv
List of Tables .....	v
Glossary .....	vi
Executive Summary .....	vii
Abstract .....	1
1. Introduction .....	1
2. Waste Packages and Processes Affecting Waste Package Performance .....	3
2.1 Waste Forms and Waste Packages .....	3
2.2 Processes Affecting the Waste Package .....	3
2.3 Earlier Programs of Similar Scope .....	5
3. PANDORA Models Description .....	8
3.1 Waste Package Model .....	8
3.2 Radiation Model .....	8
3.2.1 Source Model .....	8
3.2.2 Gamma Ray Dose Model .....	11
3.2.3 Alpha Particle Dose Model .....	14
3.2.4 Spontaneous Fission and Neutron Dose Model .....	14
3.3 Thermal Model .....	15
3.4 Mechanical Model .....	18
3.5 Waste Package Environment Model .....	22
3.6 Corrosion Model .....	24
3.7 Waste Form Alteration Model .....	25
3.8 Waste Transport Model .....	27
3.9 Driver Model .....	27
4. Conclusions .....	36
References .....	37
Appendix A. WAPPA's Gamma Ray Attenuation Model .....	39
Appendix B. PANDORA's Gamma Ray Dose Model .....	41

## List of Figures

2-1.	An NNWSI spent fuel container .....	4
2-2.	An NNWSI West Valley/defense high-level waste package emplaced in vertical borehole .....	5
2-3.	Alternate waste package for BWR/PWR intact spent fuel assemblies .....	6
3-1.	Geometry of example waste package model .....	9
3-2.	Data flow diagram of radiation model .....	10
3-3.	Cross-sectional view of a cylindrical waste form .....	13
3-4.	Temperature profile to transfer heat generated in an annulus .....	17
3-5.	The most common water flow pattern .....	23
3-6.	Simplified modeling strategy assumes water flux is led into borehole .....	23
3-7.	Data flows, data stores, and grouped inputs and outputs .....	28
3-8.	Data flow symbols and conventions .....	29
3-9.	Data flows for radiation, thermal, and mechanical stress processes .....	31
3-10.	Data flows for waste package environment and corrosion rate processes .....	32
3-11.	Data flows for corrosion increment process .....	32
3-12.	Data flow diagram combining processes shown in Figs. 3-9 through 3-11 .....	33
3-13.	Data flow diagram showing the "mechanical or corrosion failure modes" process .....	34
3-14.	Data flow diagram for the waste form alteration and waste transport processes .....	35
A-1.	Output from WAPPA's gamma ray attenuation model .....	39
A-2.	Geometry for Rockwell's attenuation model .....	40
B-1.	Mass energy absorption coefficient for gamma rays .....	42
B-2.	Cross-sectional view of a cylindrical waste form .....	43

## List of Tables

3-1.	Elements of the data dictionary for Fig. 3-2 .....	11
3-2.	Loads included in the mechanical model .....	18
3-3.	Mechanical topics deferred for future consideration .....	18
3-4.	Mechanical element types .....	18
3-5.	Elements of the data dictionary for Fig. 3-9 .....	30
3-6.	Data dictionary elements added for Fig. 3-10 .....	30
3-7.	Data dictionary elements added for Fig. 3-11 .....	30
3-8.	Data dictionary elements added for Fig. 3-13 .....	33
3-9.	Data dictionary elements added for Fig. 3-14 .....	35

## Glossary

2-D	Two-dimensional.
annulus	A cylindrical solid with a hollow center.
BWR	Boiling water reactor.
CFR	Code of Federal Regulations.
Computer Codes:	
BARIER	For waste package performance assessment; published by Stula et al. (1980).
MORSE-L	For gamma ray and neutron penetration and attenuation; Wilcox (1972).
ORIGEN2	For buildup and decay of fission products and other radioactive products; Croff (1979).
PANDORA	Performance Assessment of NNWSI Waste Package Design Omitting Random Aspects; this report.
TACO2D	For heat transfer; Burns (1982).
TOUGH	For coupled heat and groundwater movement; Pruess and Wang (1984).
WAPPA	For waste package performance assessment; INTERA (1983).
DB	Data base.
DHLW	Defense high-level waste.
DOE	U.S. Department of Energy.
EBS	Engineered barrier system.
EPA	U.S. Environmental Protection Agency.
Inconel	A series of iron-nickel alloys.
INTERA	INTERA Environmental Consultants, Inc.
LLNL	Lawrence Livermore National Laboratory.
MTHM	Metric ton of heavy metal (thorium, uranium, and heavier elements).
NNWSI	Nevada Nuclear Waste Storage Investigations.
NRC	U.S. Nuclear Regulatory Commission.
O.D.	Outer diameter.
PWR	Pressurized water reactor.
SCP	Site Characterization Plan.
t/h	Time history.
WP	Waste package.
WV/DHLW	West Valley/defense high-level waste.
Zircaloy	A series of zirconium alloys used as nuclear reactor fuel cladding.

## Executive Summary

A candidate repository site at Yucca Mountain, Nevada, is being evaluated for permanent disposal of high level nuclear waste and spent fuel. This work is being carried out by the Department of Energy's (DOE) Nevada Nuclear Waste Storage Investigations (NNWSI) project under the direction of DOE's Office of Civilian Radioactive Waste Management. The design and performance verification of waste packages for the NNWSI Project has been assigned to the Lawrence Livermore National Laboratory (LLNL).

Integrated assessments of the performance of waste package designs must be made in order to qualify waste package designs with respect to the containment time and release rate requirements set by the U.S. Nuclear Regulatory Commission (NRC) in the Code of Federal Regulations, Chapter 10 60. It is also necessary to calculate releases to the accessible environment; to accomplish this, a source term of releases from the waste package as a function of time must be provided to the total repository system performance assessment.

The waste package is one component of the system of engineered and natural barriers intended to contain and isolate the radioactive waste. The NRC performance criteria for the engineered barrier system have been adopted by DOE as design goals for the waste package. The performance measures for these design goals are:

1. Time to loss of essentially complete containment.
2. Maximum annual release rate of each radionuclide from the waste package.

The annual release rates of radionuclides, as a function of time, will be provided to the total repository system performance assessment. For times up to 10,000 years and 100,000 years after repository closure, the cumulative amounts of radionuclides released will also be calculated.

The performance of the waste package is affected by many processes acting in an interrelated manner over a long time duration. Given this complexity and duration, long-term assessments will necessarily be based on computational models. It is the task of performance assessment to construct, link, and validate these computational models and then to analyze waste package designs to demonstrate that selected designs perform as required. These analyses will also guide the design process by allowing comparison of alternative waste package designs. Such models can help determine the sensitivity of performance to environmental and design parameters. These models can also evaluate the envelope of environmental conditions that the individual waste package may experience.

We plan to develop our performance evaluation model and program iteratively in several generations. This report outlines our approach and describes both the phenomena and our first generation of conceptual models, which will be implemented in the performance assessment computer code PANDORA (Performance Assessment of NNWSI Design Omitting Random Aspects). Thus, the report documents the conceptual model development and provides a specification for the computer code. We will develop a second series of computer programs to assess the reliability of waste package performance.

We model the processes separately as far as possible and then couple these models through an explicit set of data transfers. (These data transfers and their timing and logic are represented in a driver model). We purposely simplify the process models in order to enhance the integrated

model's feasibility, speed, and clarity. Detailed models focusing on one or two processes are available or are being developed within the LLNL Waste Package Task. These detailed models can be used to calibrate the degree of approximation of the simpler models in the system model.

The purposes of the first generation of model and code development are (1) to guide later generations of development and (2) to get first-approximation results that examine interactions among the processes and evaluate proposed designs.

Our conceptual models use present knowledge and indicate an agenda for future information needs. The radiation source, radiation attenuation, thermal, and mechanical processes are understood in some detail. Future needs in these areas include modeling of effects near the ends of the waste package, validating simplified models, and evaluating the achievable values in the simplification-accuracy trade-off.

The groundwater flow details near the waste package are presently unknown for the proposed emplacement geometry and the unsaturated, thermally changing conditions. Our greatly simplified model is conservative, possibly by orders of magnitude.

We include general corrosion in the first model but defer localized corrosion modes, such as pitting and stress corrosion cracking. It is unclear whether we can model these modes by establishing conservative bounds on go/no-go thresholds or whether we will need models including microscopic initiation and subcritical growth over the long time period of interest to waste package performance.

We model waste form alteration and transport of waste to the waste package boundary by data tables to be developed from experiments. When the details of groundwater movement through a partially degraded waste package are developed, the corresponding responses of waste form alteration and waste transport processes may require more detailed models to describe the range of possible flow patterns and responses.

Our first generation computer code will be able to examine the interactions of processes affecting the waste package. Included in the first generation model are interactions among heat source, heat transfer, fluid flow, mechanical stress, and general corrosion. Gamma radiation effects on corrosion can be included via data tables. The magnitudes of different radiation types—gamma rays, alpha particles, spontaneous fissions, and neutrons—will be calculated over time; their relative magnitudes can guide modeling of their effects in later generations of the model. We will calculate the first-order effects of progressive degradation of barriers upon fluid flow. We will also calculate the effects of fluid flow, temperature, and radiation upon waste form alteration and waste transport to the boundary of the waste package.

Calculations with the first generation computer code will quantify some (but not all) of the important consequences of design choices. Calculations will also indicate which of the modeled processes and interactions are most important. Calculations of magnitude of effects and sensitivity, and estimates of uncertainty or suspected bias (hopefully in a conservative direction) can identify present model simplifications most in need of refinement in the next generation model.

# Waste Package Performance Assessment: Deterministic System Model Program Scope and Specification

## Abstract

Integrated assessments of the performance of nuclear waste package designs must be made in order to qualify waste package designs with respect to the containment time and release-rate requirements set by the NRC in the Code of Federal Regulations (10 CFR 60). PANDORA is a computer-based model of the waste package and of the processes affecting it over the long term, specific to conditions at the proposed Yucca Mountain, Nevada, site. The processes PANDORA models include: changes in inventories due to radioactive decay, gamma radiation dose rate in and near the package, heat transfer, mechanical behavior, groundwater contact, corrosion, waste form alteration, and radionuclide release. The model tracks the development and coupling of these processes over time. The process models are simplified ones that focus on major effects and on coupling. This report documents our conceptual model development and provides a specification for the computer program. The current model is the first in a series. Succeeding models will use guidance from results of preceding models in the PANDORA series and will incorporate results of recently completed experiments and calculations on processes affecting performance.

## 1. Introduction

A candidate repository site at Yucca Mountain, Nevada, is being evaluated for permanent disposal of high level nuclear waste and spent fuel. This work is being carried out by the Department of Energy's (DOE) Nevada Nuclear Waste Storage Investigations (NNWSI) project under the direction of DOE's Office of Civilian Radioactive Waste Management. The design and performance verification of waste packages for the NNWSI Project has been assigned to the Lawrence Livermore National Laboratory (LLNL).

Integrated assessments of the performance of waste package designs must be made in order to qualify waste package designs with respect to the containment time and release rate requirements set by the NRC in 10 CFR 60. It is also necessary to calculate releases to the accessible environment; to accomplish this, a source term of releases from the waste package as a function of time must be provided to the total repository system performance assessment.

The waste package is one component of the system of engineered and natural barriers intended to

contain and isolate the radioactive waste. The licensing process under 10 CFR 60 requires that two basic criteria be met by the Waste Package and Engineered Barrier System (EBS) after repository closure:

1. Substantially complete containment for 300 to 1,000 years after permanent closure of the repository.
2. Release of any radionuclide not to exceed one part in 100,000 of the 1,000 year post-closure inventory of that radionuclide, per year, for a period consistent with the applicable Environmental Protection Agency standards for radioactivity (now defined to be 10,000 years by EPA regulations in 40 CFR 191). This limit does not apply to any radionuclide released at a rate less than 0.1% of the calculated limit on total release rate. (The calculated limit on total release rate is taken to be one part in 100,000 per year of the total inventory of radioactive waste in Curies remaining 1,000 years after emplacement.)

The performance criteria for the engineered barrier system have been adopted by DOE as design goals for the waste package. The performance measures for these design goals are:

1. Time to loss of containment.
2. Release rates of radionuclides from the waste package after containment failure.

These measures become the criteria by which various waste package designs will be analyzed. We will calculate the annual release rates of radionuclides, as a function of time, for use in total repository system performance assessment. We will take the maximum over time of these release rates of radionuclides from the waste package to compare with the NRC release rate criterion on the engineered barrier system. We will also calculate the cumulative amounts of radionuclides released, for times up to 10,000 years after repository closure, to compare with EPA limits in 40 CFR 191, and for times up to 100,000 years to allow a comparison among candidate sites as provided in DOE regulations in 10 CFR 960.

The performance of the waste package is affected by many processes acting in an interrelated manner over a long time duration. Given this complexity and the long periods discussed in the criteria above, long-term assessments will necessarily be based on computational models. It is the task of performance assessment to construct, link, and validate these computational models and then to analyze waste package designs to demonstrate that selected designs perform as required. These analyses will also guide the design process by allowing comparison of alternative waste package designs. Such models can help determine the sensitivity of performance to environmental and design parameters. Further, integrated performance calculations may indicate that the current envelope of test conditions for the individual waste package processes requires expansion or allows reduction.

We outline our modeling approach and describe the phenomena and the corresponding models, which we will implement in a performance assessment computer code, PANDORA. Thus, we document the conceptual model development and provide a specification for the computer code. The specification states what the program will do; describes the models by concepts, equations, or narratives; and identifies essential output information.

We plan to develop our performance evaluation model and program in several generations. The present first-generation model has simple models of most

of the important processes affecting the waste package and couples them so as to track their interactions over time and to evaluate the performance measures of the waste package. Our purpose is to acquire (1) first-approximation results for the uses mentioned earlier and (2) a guide to the development of later generations of the program. Later generations will be more detailed and accurate and will incorporate new information developed by the NNWSI testing series and any new features needed to model later reference designs of waste packages. A second series of our computer programs will examine the reliability of the waste package performance. The first series of programs are deterministic in their character; they can serve as a core or a guide for the probabilistic reliability programs.

We are following an orderly method of computer program development. The phases are to scope, specify, design, implement, and test the program. Each phase produces a product which can be reviewed. Reviews are planned after the specification, design, and test phases. Iterations on the development phases will be conducted as necessary. In this report, for the first-generation program we combine the products of the first two phases—the scope or charter and the specification. The specification states what the program must do. In the next phase—design—we will consider solution methods to specified problems, program structure into subroutines, and program control and data structures.

Our system modeling approach is to model the processes separately as far as possible and then to couple these models through an explicit set of data transfers. These data transfers and their timing and logic are represented in a driver model. The process models are purposely simplified to enhance the integrated model's feasibility, speed, and clarity. Detailed models focusing on one or two processes are available or are being developed within the LLNL Waste Package Task. These detailed models can be used to calibrate the degree of approximation of the simpler models in the system model.

In the following sections we describe the principal processes affecting the waste package's long-term performance (Sec. 2) and the models developed for these processes (Sec. 3). The identification of the principal processes is already a modeling step in that it involves selection—choosing the important processes and factors, and not choosing those deemed to be secondary or irrelevant.

## 2. Waste Packages and Processes Affecting Waste Package Performance

### 2.1 Waste Forms and Waste Packages

Detailed descriptions of the waste package designs, materials, anticipated environments, and processes affecting the waste package over the long term will be presented in Chapter 7 of the NNWSI Site Characterization Plan (SCP). In this section we present a thumbnail sketch of the waste packages, and in Sec. 2.2 we describe the processes affecting them. Based on the descriptions, data bases, and evaluations in the SCP, we developed models of the packages and processes. We describe these models in Sec. 3.

The waste package designs and alternate designs are described in SCP Section 7.3. PANDORA should be capable of modeling the waste package designs and variations on the designs. Some NNWSI waste package designs are illustrated in Figs. 2-1 through 2-3. The waste forms are (1) spent nuclear fuel and (2) high-level waste solidified in a glass matrix. The spent fuel rods may be in assemblies as removed from the reactor, or they may be consolidated into a smaller volume (see Fig. 2-1). In the latter case, the assembly hardware may be packed in the center of the waste package. West Valley and defense high-level waste (WV/DHLW) will be immobilized in a glass pour canister which is placed in a second container (Fig. 2-2).

Some designs include an emplacement-hole liner of steel. In the case of horizontal emplacement, there may also be a dolly to roll or slide the waste packages into place and to support them approximately centered in the liner; at present, details of design are not final. Alternate designs under consideration include different dimensions and packing geometries (Fig. 2-3) and different container metals or alloys.

### 2.2 Processes Affecting the Waste Package

In this section we identify the processes affecting the long-term performance of the waste package. We describe these processes in more detail in Sec. 3, in conjunction with our discussion of the models. We summarize the interactions and feedbacks of these processes in Sec. 3.9.

The containment function is provided by a sealed metal container or by several containers inside one another. Failure of complete containment of waste requires loss of container integrity and a means to move waste out. We use time to loss of barrier integrity as a lower bound on time of loss of containment.

The loss of barrier integrity can develop by either mechanical means (e.g., rupture due to stress) or chemical means (e.g., uniform corrosion, stress corrosion cracking, or pitting corrosion). The processes leading to loss of barrier integrity are influenced by the nearby external environment (e.g., rock failures causing localized stress on the waste package) and by groundwater flow. The processes are also influenced by the internal environment interacting with the external environment. Examples include (1) the heat generated by the radioactive waste being transferred to the external rock, thus establishing the temperature field; and (2) gamma radiation being generated by the waste and attenuated by the waste and by metal barriers, thus producing a net gamma ray flux at the surfaces of the metal barriers. The gamma ray flux can cause radiolysis in the water which might then increase the corrosion rate.

For spent fuel, the Zircaloy cladding can provide an additional barrier for containment of the fuel pellets and, even when partially breached, can help limit the rate of release of the waste. A small part of the spent fuel radioactive waste consists of activated elements in the Zircaloy itself and in the stainless steel framework of the fuel assemblies; for these waste components the cladding does not provide an additional barrier.

The time to loss of barrier integrity is a lower bound on the time to loss of containment. Most radionuclides require water for mobilization from the waste form matrix and for transport. Gaseous radionuclides can move by diffusion in air.

The processes leading to loss of integrity of the waste package barriers can be listed in summary as:

1. Radiation
  - Gamma ray source
  - Gamma ray attenuation
  - Heat source.
2. Thermal
  - Heat transfer, temperature field.
3. Mechanical
  - Loads
    - External (pressure or localized force)
    - Internal pressure
    - Thermal expansion in the established temperature field
    - Stresses in static balance.
  - Modes of possible change or failure
    - Yielding
    - Ductile rupture
    - Brittle rupture from a crack.
4. Waste package environment
  - Groundwater flow/thermal effects

- Groundwater chemistry
- Flow mechanisms of water-contact with the waste package.

5. Corrosion

- Corrosion modes in presence of either steam, water vapor, partial saturation of liquid water, or unexpected full saturation.
  - Uniform corrosion
  - Stress corrosion cracking
  - Pitting corrosion
  - Galvanic corrosion
  - Other corrosion modes.

Some of the processes are continually in a static equilibrium. With some time-lag exception during the first few years after emplacement, the temperature distribution is essentially in equilibrium with the heat generation, which changes very slowly. The stress distribution forms a static equilibrium with the internal and external forces. Some processes cause gradual changes, e.g., reducing barrier thickness by corrosion. Some processes cause abrupt and discrete changes, e.g., perforation of a barrier due to mechanical rupture or due to corrosion penetrating the full thickness of the barrier.

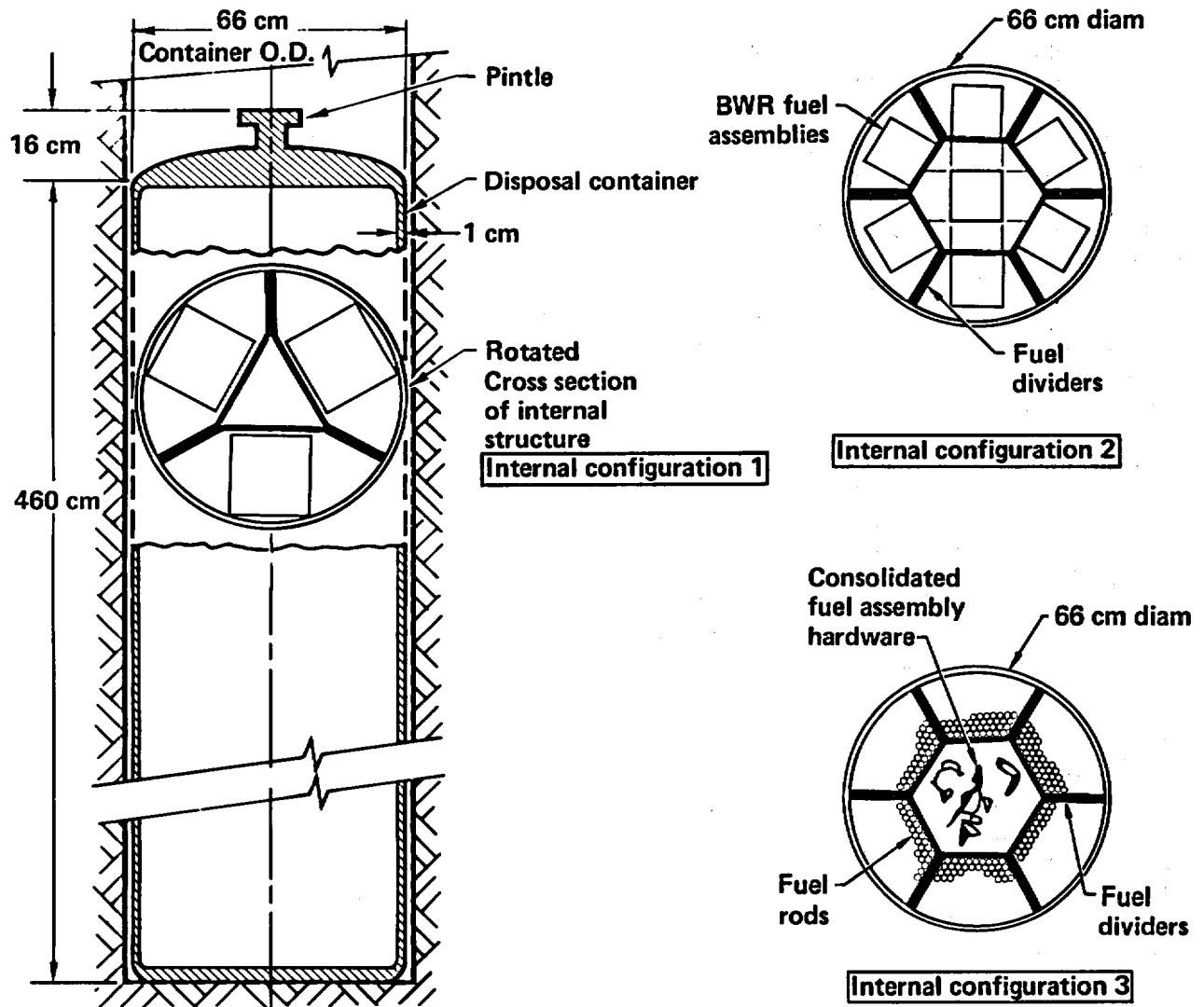


Figure 2-1. An NNWSI spent fuel container, with alternate internal configurations supported by space dividers. Configuration 1: three intact PWR assemblies. Configuration 2: seven intact BWR assemblies. Configuration 3: fuel rods consolidated from 6 PWR or 12 BWR assemblies; assembly support hardware is consolidated in the central zone of the waste package (details not to scale).

The existence and rate of waste release from the waste package are dependent on three processes:

1. Existence of a breach of the barrier, opening a potential path between the waste form and the external medium.
2. Alteration of the waste form, converting some part of the waste into mobile form.
3. Transport of the mobile waste from the waste form to the external medium (the rock around the borehole).

The major part of the waste is in the spent fuel's uranium-oxide matrix fuel pellets or in the glass matrix for reprocessed waste. This waste is altered to

a mobile form as the waste and matrix go into solution in groundwater. The transport is then through or with groundwater. For the spent fuel, there are a few exceptions, which we discuss in Sec. 3: (a) some radioactive elements due to activation of structural materials in the Zircaloy cladding and the assembly framework; (b) some elements released in gaseous form, principally carbon-14 as CO<sub>2</sub> and noble gases; and (c) the fraction localized in the pellet-cladding gap and in matrix grain-boundaries.

The rate of waste form alteration depends on the amount and duration of groundwater contact with the waste form, which in turn depends on the groundwater flow and on the waste container condition: i.e., one small breach, several small breaches, many breaches, or total dismantlement. The rate of waste form alteration may also depend on temperature, water chemistry, gamma ray dose rate at the waste form/water interface, and accumulated waste form material damage due to alpha decays and spontaneous fissions within the waste form. The rate of waste form alteration will also depend on the rate of mobile waste transport away from the waste form/water interface.

The mobilized waste may increase the gamma radiation flux near the barrier surface, thereby increasing the rate of corrosion of the breached barriers. However, this is not expected to be an important factor because (1) the radiation source strength will be low by the time the barriers become breached, and (2) only a small fraction of the waste will be in mobile form in the waste package volume.

In summary, the processes affecting the rates of waste form alteration and waste release from the waste package include most of those given for barrier failure, plus the following:

1. Radiation
  - Alpha radiation (and spontaneous fission) source
  - Alpha (and fission) integrated quantities.
2. Waste form alteration
3. Transport of mobile waste.

PANDORA examines these processes and their interactions. In Sec. 3 we discuss in more detail the controlling factors (inputs) and the interactions among processes, as well as the models developed to represent these processes.

### 2.3 Earlier Programs of Similar Scope

Earlier computer programs of comparable intent are BARIER (Stula et al., 1980 and WAPPA (INTERA, 1983). These are waste package systems codes that have relatively simple models of each

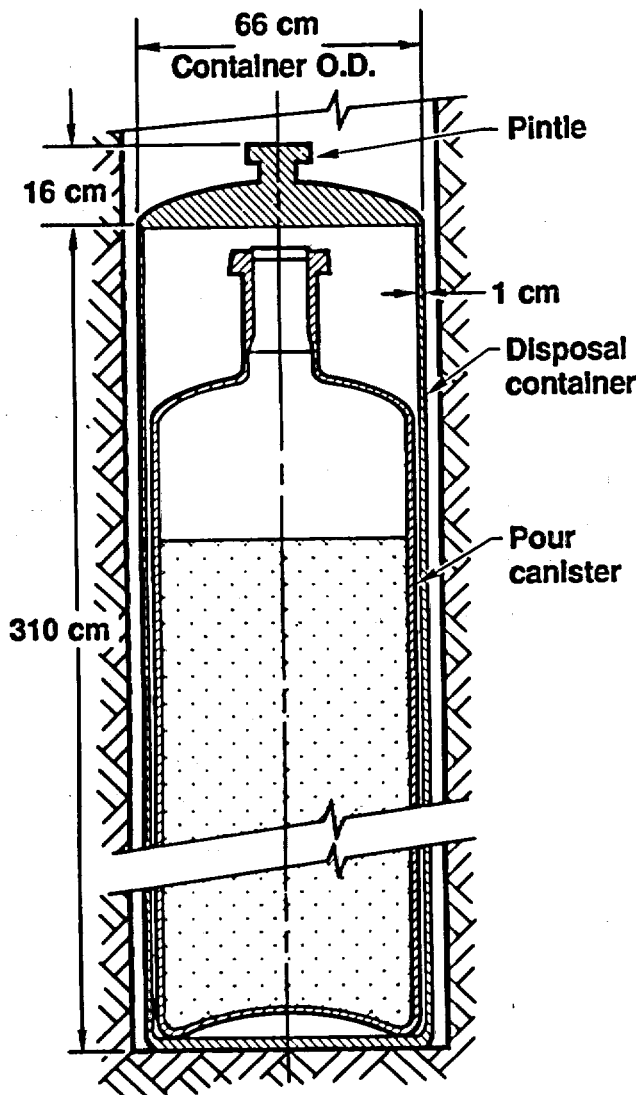


Figure 2-2. An NNWSI West Valley/defense high-level waste package emplaced in a vertical borehole.

process and treat the interactions of the processes over time.

We have examined and tested WAPPA for possible application to the NNWSI waste package. WAPPA provides a good starting "shopping list" of phenomena and concerns that should be examined. However, we find that many of the models and assumptions in WAPPA, although applicable to other conditions, are not applicable to the NNWSI waste package design and the environment in the repository. In the following paragraphs we summarize the conceptual problems, but we do not intend to provide a complete review of WAPPA's theory and implementation.

**Waste Package.** WAPPA's geometry is one-dimensional with cylindrical symmetry and no axial

variation. The waste form is the central cylinder and is monolithic. We also plan to use the simplifying assumption of no axial variation. However, for spent fuel, if we treat the Zircaloy cladding as a supplemental barrier, then we have a departure from the concept of concentric barriers around the same center point (see Fig. 2-1). Also, the spent fuel is not monolithic, and the fuel's effective volume may be a hollow cylinder instead of a filled cylinder.

**Barrier Failure by Stress Corrosion Cracking.** WAPPA contains a treatment of stress corrosion cracking (with a yes/no answer), based on an initial crack size and on an evaluation of the stress intensity at the crack tip; but the WAPPA User's Manual and the published source code listing (INTERA, 1983) do

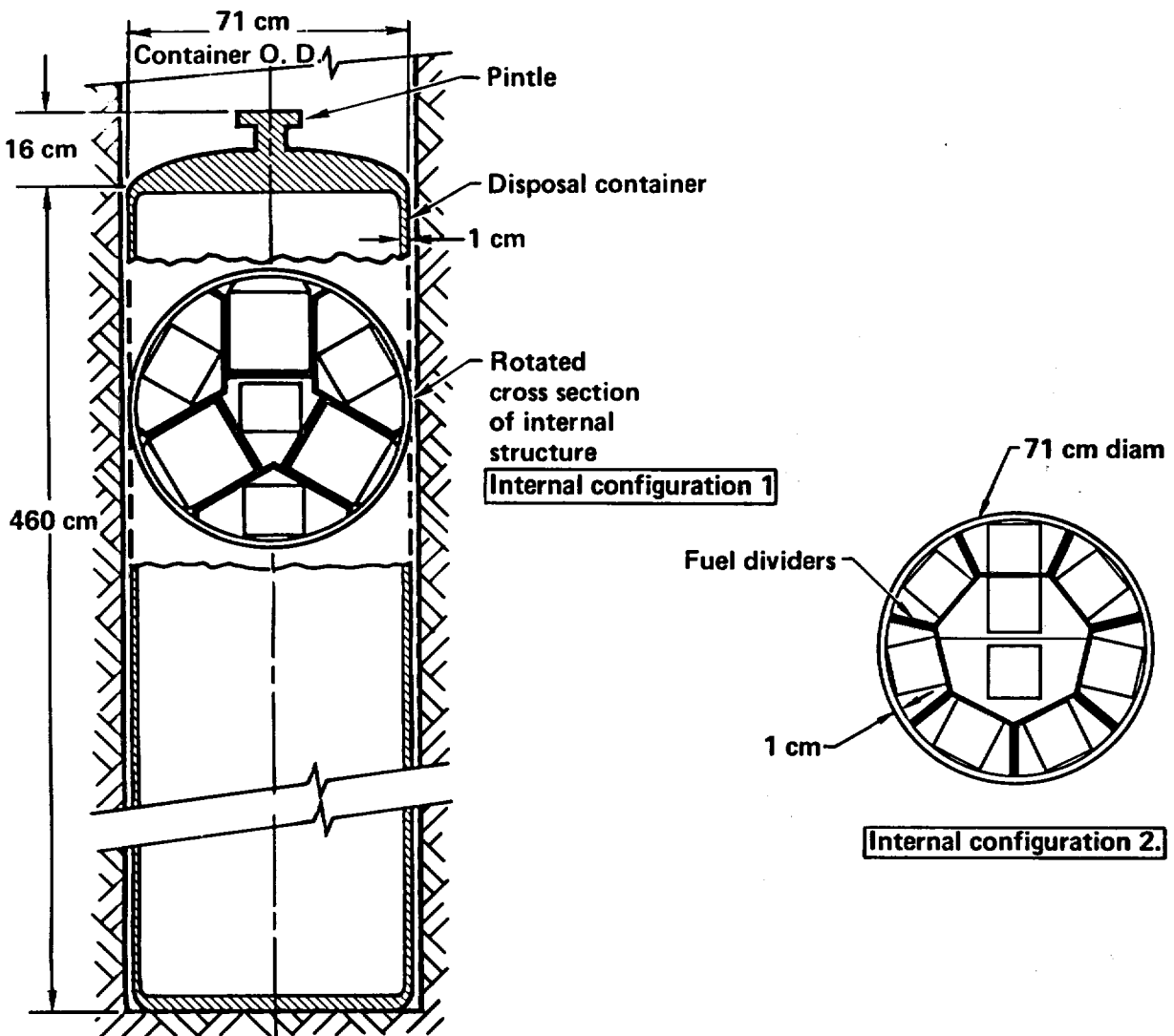


Figure 2-3. Alternate waste package for BWR/PWR intact spent fuel assemblies emplaced in vertical borehole; two alternate internal configurations for packing spent fuel assemblies.

not provide any means of input of the initial crack size. Hence, there is no way to activate stress corrosion cracking in the WAPPA code, and we are left in doubt as to whether it would work correctly if a crack size input were created. In addition, WAPPA does not model the subcritical growth of a crack.

In a salt repository with a large lithostatic pressure on the package, the barrier surface stress would be in compression rather than in tension; hence, stress corrosion cracking would not need to be evaluated. In the NNWSI repository, the tuff rock would not creep like salt. There could conceivably be minor sloughing of rock from above the borehole wall, but not enough to exert sizable pressure on the package (see Sec. 7.1 of the SCP). General corrosion would be very slow with the proposed stainless steel material of the waste package container and the mildly oxidizing conditions expected in the NNWSI repository, and other corrosion modes (such as stress corrosion cracking) would then have to be considered as the more serious possible failure modes.

**Groundwater Flow.** WAPPA treats groundwater flow by a user-input time of resaturation of the repository. There is no data structure for water flow, neither velocity nor volumetric flow rate. The NNWSI repository will be above the water table and therefore unsaturated. The groundwater flow rate will be a factor in the waste package degradation processes, even though the water flow will be in an unsaturated environment and the flow rate will be small.

**Waste Form Alteration and Waste Transport.** WAPPA assumes that diffusion through standing water controls the rate of waste form alteration and the waste form transport to the outside of the waste package geometry. This assumes a location below the water table; therefore, any opening in the waste package becomes a pathway for diffusion. This further assumes that transport of dissolved waste by moving water is negligible compared with diffusion. This last assumption may be reasonable for a situation below the water table if the waste form is surrounded by an intact backfill of a clay-like material of lower hydraulic conductivity than the surrounding rock. The NNWSI repository will be above the water table in unsaturated rock; hence, it is unlikely that there will be any continuous path for waterborne diffusion. There is expected to be some slow downward movement of water in the unsaturated rock; some of this water may contact the waste package and waste form. Therefore, both the processes and the models for waste form alteration and waste transport must be different in PANDORA than those in WAPPA.

**Gamma Ray Attenuation.** Gamma ray attenuation between the waste form surface and the package surface will not be very great in the NNWSI reference package design because of the relatively thin wall in this design. Nonetheless, for completeness we note that WAPPA's gamma ray attenuation model has a conceptual error and a reliance on extrapolated data. One of the parameters of their referenced model is taken as a constant in WAPPA, but it is a variable in the original reference dependent on radial distance from the waste form centerline. The reference determines the value by a graphical lookup. More detail is deferred to Appendix A. The same conceptual model and error are found in BARRIER. The model requires "buildup factor" data that are unavailable for the cylindrical geometry of interest and must be taken from data measured in plane geometries.

**Time Sequencing of Processes and of Failure Modes.** WAPPA's "Driver" model evaluates the waste package condition at a sequence of user-input time points. We wish to find the approximate time of container failure. With WAPPA this requires iterated computer runs with new user-defined time points.

At each user-input time point, WAPPA evaluates the processes in the following order:

- Radiation
- Thermal
- Mechanical
- Corrosion

Waste form alteration and waste transport.

Groundwater flow is treated by a user-input time of resaturation of the repository. If a mechanical stress has exceeded some yield- or breach-threshold at this time point (i.e., crossed the threshold some time in the preceding time interval), then the package change-of-condition is recorded and the mechanical evaluation is reiterated. If a corrosion process has caused a breach during the preceding time interval, then the package change-of-condition is recorded and the corrosion evaluation is reiterated. The WAPPA approach might give reasonable results if the time steps are small during critical intervals before major changes in the package condition. It is the user's responsibility to specify the time points. Accuracy would usually require iterated computer runs. We feel it is better to start afresh from the requirements definition phase rather than fully identifying and verifying WAPPA's time sequencing approach, and possibly modifying it for ease of use.

### 3. PANDORA Models Description

PANDORA must treat the waste packages and processes described in Secs. 2.1 and 2.2. The model geometry for an appropriate degree of simplification has essentially one dimension of variation, the radial direction in a cylindrical geometry. There are seven process models:

1. Radiation model
2. Thermal model
3. Mechanical model
4. Waste package environment model
5. Corrosion model
6. Waste form alteration model
7. Waste transport model (covering transport within the waste package system).

Each model may consist of several interacting or thematically related submodels. The time characteristics of the processes (as noted in Sec. 2.2) are diverse. In Secs. 3.1–3.8 we describe the individual models. In Sec. 3.9 we describe the driver model, which treats the interactions of the models and the sequencing of these interactions.

#### 3.1 Waste Package Model

The waste package model describes the initial geometry and properties of the package and keeps track of the current conditions of the waste package as time moves along. We assume a cylindrical geometry with variability only in the radial direction. Because of the large length-to-radius ratio of the waste packages, an assumption of axial uniformity seems suitable over most of the length of the waste package. Cylindrical symmetry seems suitable in most cases (see Sec. 2.1), but its use for some cases of spent fuel assemblies (see Figs. 2-1 and 2-3) is a coarser degree of approximation and will require comparison with two-dimensional calculations.

Each annular element in the waste package is described by its inner and outer radii and a material name keyed to a data base of material properties (see Fig. 3-1, modeled on Fig. 2-1 Configuration 3). For each metallic barrier or borehole liner, PANDORA will add corrosion-layer annuli. (Corrosion products may accumulate or be carried away, depending on conditions and on the corrosion data-base inputs.) PANDORA will add a gas gap annulus wherever there is a void between solid annuli. A narrow gap may close or open up as a result of differential thermal expansion or corrosion-layer buildup. The properties of waste-form annuli may be space-averaged proper-

ties, actual properties of the solid waste form, or total quantity per waste package. We use space-averaged properties in these models: gamma ray source rate, gamma ray attenuation, heat generation, heat transfer, and mechanical effects. We use actual density in the alpha particle dose rate and accumulated dose models. We use the total quantity of each type of waste in each annulus (per package) as baseline inventories in the waste form alteration and waste transport models.

The Zircaloy cladding can serve as an additional barrier protecting the spent fuel waste form. This barrier does not have the common radial center of the outer barrier(s), but it does have the logical relation of one barrier within another. In the input data structure we will tabulate the waste forms and barriers with their logical "contained-within-barrier" relations and their larger-scale geometric annulus location.

#### 3.2 Radiation Model

The radiation model calculates radiation sources and radiation doses in the waste package. The radiation doses may have effects on other processes; these effects will be treated within the other processes. The radiation model consists of submodels:

1. Source rates and inventory
  - Gamma ray generation rate
  - Alpha particle generation rate
  - Spontaneous fission and neutron generation rates
  - Heat generation rate
  - Radionuclide inventory.
2. Gamma ray absorbed dose rate
  - Just outside surface of waste form
  - Just outside surfaces of metal barriers.
3. Alpha particle and fission dose rates and doses
  - Within waste form
  - Just outside surface of waste form.

The first submodel involves table interpolations (in ORIGEN2-generated tables) times scaling factors. The gamma ray dose rate model is new; we discuss it in Sec. 3.2.2 and Appendix B. The submodels and their outputs and linkages are shown in Fig. 3-2 and Table 3-1.

##### 3.2.1 Source Model

This model interpolates in ORIGEN2-generated tables. ORIGEN2 (Croff, 1979) calculates the burnup

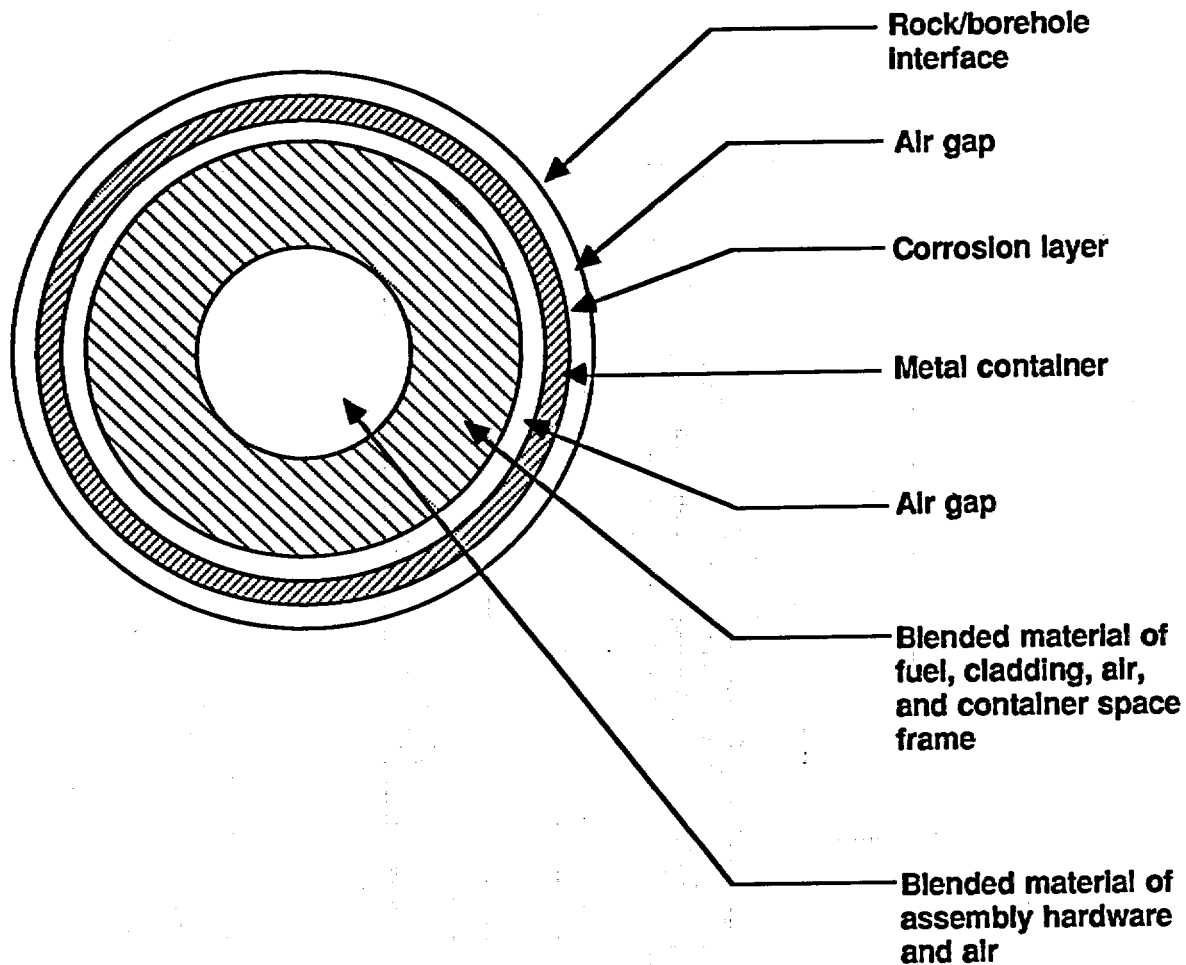


**Figure 3-1. Geometry of example waste package model.**

of nuclear fuel and the buildup and decay of fission products, activation products, and decay products during reactor operation and after the fuel has been removed from the reactor. ORIGEN2 accounts for the partitioning of elements if reprocessing is done. For our purposes, the ORIGEN2 tables provide data, as a function of time since removal from the reactor, for a unit quantity of waste derived from nuclear fuel of a specified type and burnup. The unit quantity is the amount of derived waste (or spent fuel) per metric ton of heavy metal originally in the fuel (MTHM). The source model scales from the tables' unit to the quantity of waste in the waste package.

The source model interpolates in the time variable. Most inventories and rates decrease exponentially or are sums of decreasing exponentials. Some inventories increase while products accumulate from the decay of other elements. If a quantity decreases between two time points, the model linearly interpolates the logarithm of the quantity. If a quantity increases, the model linearly interpolates the quantity.

If ORIGEN2 tables are input for several burnups, the model interpolates linearly in burnup. If ORIGEN2 tables are input for only one burnup, the model scales linearly from the tables' burnup to the waste form's specified burnup. Scaling downward from a table burnup to a waste form burnup rather than scaling upward is preferred because the inventories of actinides and of plutonium-fission products increase more than linearly with burnup.

For each annulus and for each waste form in the annulus, the source model provides these outputs:

- Heat rate [(Joules / (sec × m<sup>3</sup> of annular volume))]
- Gamma ray energy generation rate [(number × MeV) / (sec × m<sup>3</sup> of annular volume)]
- Alpha particle and spontaneous fission generation rates [number / (sec × m<sup>3</sup> of waste form's volume)]
- Inventory of each radionuclide (kg, total annular inventory).

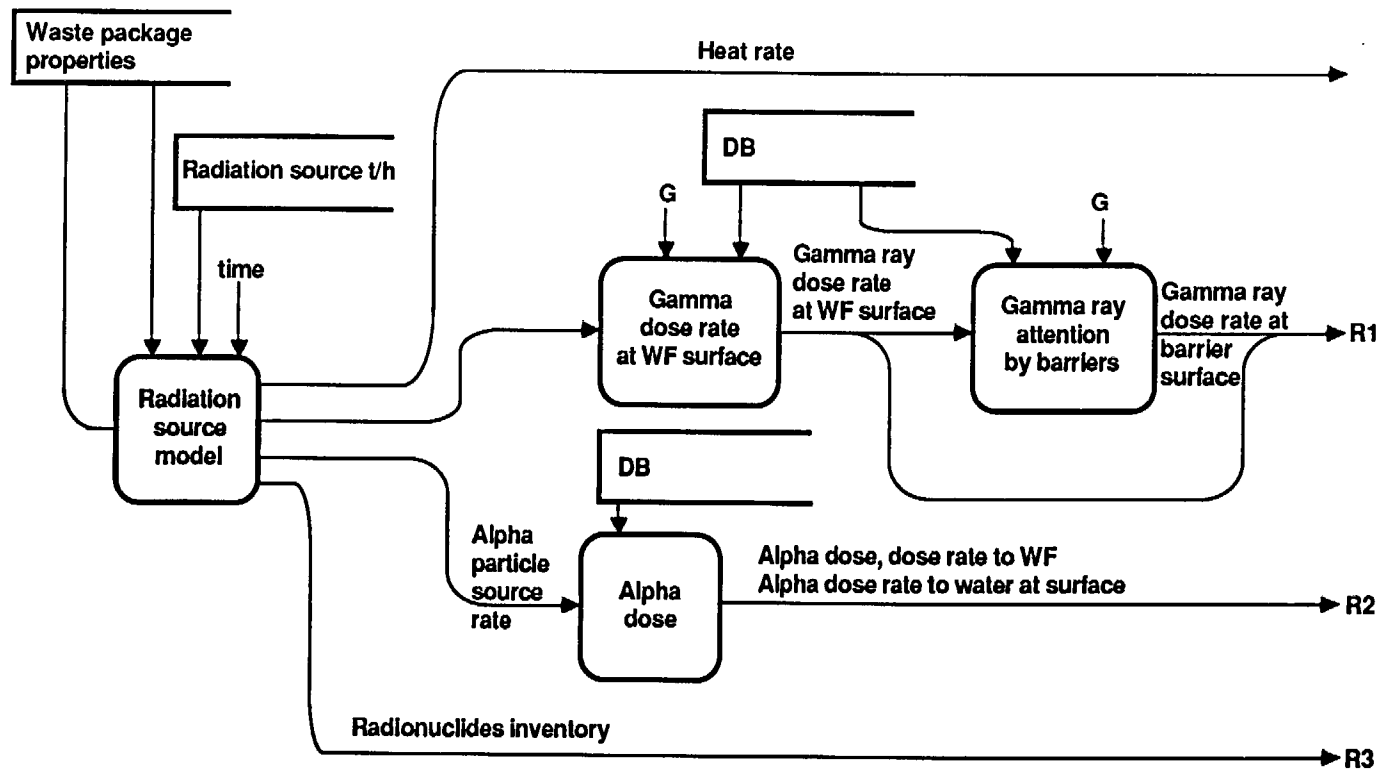


Figure 3-2. Data flow diagram of radiation model. The spontaneous fission and neutron dose model, not shown, is operationally similar to and parallel to the alpha dose model. (Symbols and terms are defined in Table 3-1.)

**Table 3-1. Elements of the data dictionary for Fig. 3-2.**

Data label	Data contents
Waste package properties	<b>Geometry</b> <b>Status of elements</b> Environment (dry/wet) Strength (Intact/yielded) Integrity (Intact/breached) <b>Material types</b> <b>Quantity of waste form</b>
G	Waste package geometry
DB	Data base of material properties
Radiation source t/h	Time history of radionuclide inventories, heat generation rate, radiation generation rate
time	Current time
Heat rate	Heat generation rate per unit volume in each waste form
Gamma ray source rate	Gamma ray energy generation rate per unit volume in each waste form
Gamma ray dose rate at WF surface	Gamma ray dose rate in water at waste form surface
Gamma ray dose rate at barrier surfaces	Gamma ray dose rate in water at barrier surfaces
Alpha particle source rate	Alpha particle generation rate per unit volume in each waste form
Alpha dose rate to WF	Alpha particle dose rate to waste form
Alpha dose to WF	Alpha particle integrated dose to waste form
Alpha dose rate to water at surface	Alpha particle dose rate to water at waste form surface
Radionuclides inventory	Radionuclides inventory per waste package in each waste form
R1	<b>Radiation data:</b> Gamma ray absorbed dose rate in water at waste form surface and at surface of each barrier element
R2	<b>Radiation data:</b> Alpha particle dose rate to waste form Alpha particle integrated dose to waste form Alpha particle dose rate to water at waste form surface
R3	<b>Radiation data:</b> Radionuclides inventory per waste package in each waste form

Note that the annular volume is the annular cross-sectional area times the active length of the waste package, i.e., the length of the fuel rods or of the solid glass waste form. Using this reference volume, the heat rate and gamma ray generation rate outputs are averages over the annular cross-sectional area. For these two outputs, the source model further sums over the outputs of the waste forms contained within one annulus.

### 3.2.2 Gamma Ray Dose Model

The waste form is both a source and an attenuator of gamma rays. The metal barriers are attenuators of gamma rays. When water is present at the surface of a barrier or waste form, we want to compute the gamma

ray absorbed dose rate in water because this causes radiolysis in the water, which may cause enhanced corrosion of the metal barrier or enhanced alteration of the surface of the waste form.

The attenuation and the absorbed dose rate from gamma rays are complex processes. A simplified model cannot be expected to calculate the results from first principles. Rather, we need reference data from measurements or from detailed calculations.

A simplified model must, at a minimum, read a data base from a detailed calculation and scale the results over the time history of a waste package as the gamma ray source strength declines. A simplified model might also scale or adapt a few detailed results to a range of related waste forms and package designs.

We present below a simplified model and simple physical arguments indicating that our model captures the important factors for scaling and that it has a reasonable degree of accuracy. Validation of the model will require comparisons with results of the detailed calculations.

For our reference data base for the model, we use the detailed code MORSE-L (Wilcox, 1972). This calculates radiation transport using a Monte Carlo method. This code has a history of extensive use. Calculations for a spent fuel canister emplacement (Wilcox and Van Konynenburg, 1981) have been validated by measurements (Van Konynenburg, 1984).

The system-level gamma ray dose model scales or adjusts results from a MORSE-L reference calculation to a range of similar waste forms and waste package designs. Two reference results are adjusted. First, the absorbed dose rate at the waste form surface is scaled. Second, the attenuation factors between the waste form surface and the barrier surfaces are adjusted. The absorbed dose rate at the surface of a barrier is equal to the absorbed dose rate at the waste form surface times the attenuation factor.

**3.2.2.1 Gamma Ray Absorbed Dose Rate at Waste Form Surface.** We will need at least two reference calculations, one each for spent fuel and WV/DHLW. Additional MORSE-L runs must be performed to explore the degree of accuracy achievable with our model's scaling from a reference result to different waste form and waste package parameters. The following waste form features are relevant to the simplification achieved in our scaling model.

1. The waste form radii are substantially larger than the gamma ray energy absorption thicknesses of the waste form materials. That is, the waste form is a thick self-shielding source.

2. In the spent fuel case, a single spent fuel rod diameter is less than the gamma ray energy absorption thickness. A typical gamma ray passes through several fuel rods before an energy loss. Thus, we may consider the cladding, fuel pellets, and gaps between fuel rods as a blended material. (However, for a spent fuel assembly the regular spacing of fuel rods provides some nonuniformity of different directions, and this limits the accuracy of the blended-material approximation.)

3. For the constituent materials in a range of glass-matrix waste forms, the gamma ray mass energy-absorption coefficients are fairly close in value over the gamma ray energy range of interest, and these coefficients rise sharply for gamma rays below about

0.2 MeV. Any gamma rays below this energy would have a high probability of absorption and would not contribute much to the gamma ray flux at the waste form surface. The principal gamma ray energy for several hundred years is 0.66 MeV, from cesium-137.

4. For the glass-matrix waste form materials and energy range of interest, the gamma ray mass energy-absorption coefficients are fairly close in value. Thus, the absorption depends strongly on the mass density but only weakly on the percentages of the different elements constituting the waste form.

5. For spent fuel, the gamma ray mass energy-absorption coefficient is dominated by the major constituent by weight, uranium. Small changes in the fractions of the minor constituents make an even smaller change in the net coefficient for the spent fuel.

The reference calculation gives the gamma ray absorbed dose rate in water, at the surface of the waste form annulus, for a reference waste form.

For the gamma ray absorbed dose rate in water at the waste form surface, the model's scaling to a different waste form or to a different time in a waste form's history is:

1. Linear with the source gamma ray energy generation rate per unit volume, counting gamma rays above a threshold energy (to be determined, but perhaps 0.2 MeV for glass waste forms and 0.3 MeV for spent fuel).

2. Inverse with the mass density.

3. In a future program version, multiplied by a weighting factor for changes in percentages of atomic composition of the waste form.

4. Not dependent on the outer radius or inner radius.

The linear dependence on source energy generation rate above the threshold is as follows: if the number of gamma rays per second increases while average energy per gamma ray is fixed, then the total energy and the dose rate increase with the number. If the average energy per source gamma ray increases while the number per second is fixed, then the energy flux increases. There is little change in the fraction of energy absorbed from this energy flux, as a function of energy. We discuss energy absorption in Appendix B.

The inverse dependence on mass density is as follows: as mass density increases, the attenuation of the energy flux increases, so the energy flux exiting the waste form decreases. We present our full argument in Appendix B.

For a future model version, we could refine this mass density dependence by using a factor dependent on the mass fractions of different atomic number

elements in the waste form, weighting each mass fraction by its gamma ray mass energy-absorption coefficient at a selected gamma ray energy (see Appendix B).

The lack of dependence on radius can be seen by reference to Fig. 3-3. Because of the self-shielding effect and because the point of observation is at the surface of the waste form, an increase in radius has very little effect on the extent of source region visible to the point of observation. Hence, the flux per unit area and the absorbed dose rate per unit volume are virtually unchanged.

The scaling above applies at the outer surface of a waste form. For the spent fuel case, interior fuel rods as well can eventually be exposed to water and to alteration processes. At an interior location, the gamma ray absorbed dose rate in water is approximately twice the rate at the exterior surface; the model assumes exactly twice. An interior point can be thought of as being within a sandwich of sources. The interior point gets irradiated from both sides (all angles), while the surface point gets irradiated from only one side (from one hemisphere of angular directions).

There may be more than one waste form annulus in a waste package—see for example Fig. 2-1 Configuration 3. Our model reduces the added complexity

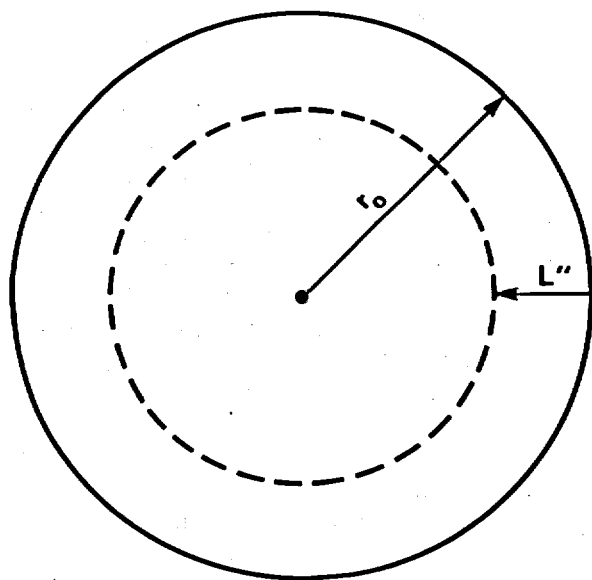


Figure 3-3. Cross-sectional view of a cylindrical waste form with radius  $r_0$ . Most of the gamma ray energy originating in the deep interior is absorbed.  $L''$  is defined as follows. Half of the gamma ray energy exiting the waste form surface originates from the zone within a depth  $L''$  from the surface.  $L''$  is less than  $L_{en}$  (see Appendix B).

by assumptions. The model assumes that the outermost waste form annulus is a thick self-shielding source; the dose rate at its outer surface comes from that source alone. An inner waste form annulus is not necessarily thick to gamma rays. The absorbed dose rate at both the outer and interior surfaces of the inner annulus is taken to be the larger of (1) its own interior-surface dose rate as calculated by the one-source model and (2) the outer annulus' interior-surface dose rate.

In summary, the output of the model for the gamma ray absorbed dose rate at the surface of the waste form annulus is:

- Gamma ray absorbed dose rate in water, at waste form outer surface (Gy/sec).
- Gamma ray absorbed dose rate in water, at waste form inner surfaces (Gy/sec).\*

**3.2.2.2 Gamma Ray Attenuation—Gamma Ray Absorbed Dose Rate at Waste Package Element Surfaces.** The gamma ray energy flux is attenuated by the intervening material between the waste form surface and an outer location such as a metal barrier surface. Hence, the absorbed dose rate in water from this flux also decreases with the intervening material. The attenuation of absorbed dose rate depends on the amount and the atomic numbers of the material. The attenuation also depends on the geometry of placement of this material and on material outside this direct path which can scatter gamma rays back toward the point of observation. In the waste package case, the attenuation also depends on a purely geometrical factor—the increase in area of a cylindrical surface as the radius  $r$  increases. This last factor gives a  $(r_0/r)$  dependence of the flux and absorbed dose rate in the absence of any intervening material. ( $r_0$  is the radius of the waste form. The mass factor dominates over the  $r_0/r$  dependence unless the mass is a gas.)

The model adjusts attenuation factor results from one MORSE-L reference calculation. The absorbed dose rate in water at any location in the reference calculation is a factor (the attenuation factor) times the absorbed dose rate in water at the waste form surface. When we divide out the  $r_0/r$  dependence, the remaining factor is assumed to depend only on the absorbing material.

For an input-specified waste package and any specified location, we calculate the mass thickness along a line from the waste form surface to the point of

\*Absorbed dose is the energy imparted to matter by ionizing radiation, per unit mass of the matter. The unit, one Gray (Gy), is one Joule/kg. The Gray replaces the rad; 1 Gy = 100 rads.

observation ( $\text{kg}/\text{m}^2$ ). (If necessary, we multiply the mass thickness by a weighting factor for different atomic numbers— please see the next paragraph.) Next, we look up the attenuation factor in the reference calculation for the same mass thickness (which may have been reached at a different radius). Then we factor in the  $r_o/r$  dependence for the radius  $r$  in the input-specified package. The resulting number is the attenuation factor for the absorbed dose rate in water from the waste form surface to the point of observation.

If the absorbing mass in the reference waste package and in the input-specified waste package have the same fractions of different elements, or if the elements are all in the atomic number range from oxygen to copper, then no weighting factor is needed. But if there is a wider range of atomic numbers and the fractions differ, then weighting factors are used on each of the two mass thicknesses. The weighting factor is the sum (over atomic elements) of the mass fraction of that element (in the mass between the waste form surface and the point of observation) times that element's gamma ray mass energy-absorption coefficient (at a selected gamma ray energy).

Changes in geometry of absorbing material placement, from the waste package in the reference calculation to other waste package designs, are expected to be limited enough that we can adapt the reference calculation using only the material thickness and radius factors just described.

In cases with more than one waste form annulus, the gamma ray absorbed dose rate at an outer barrier surface is calculated from a source consisting of the outermost waste form annulus alone. The gamma rays from inner waste form sources are assumed to be shielded out by the mass of the outermost waste form.

In summary, the output of the model for the absorbed dose rate at waste package element surfaces is:

- Gamma ray absorbed dose rate in water at the specified surfaces ( $\text{Gy}/\text{sec}$ ).

### 3.2.3 Alpha Particle Dose Model

Alpha decays can cause atomic displacement defects in the solid waste form and can irradiate a water layer (if present) at the surface of the waste form. When an atomic nucleus decays by alpha particle emission, the alpha particle and the recoiling residual nucleus cause a number of atomic displacements in the solid material. A number of these displacement defects remain locked in the solid. The defects accumulate, although there is a saturation effect. The solid with defects may be more easily altered when exposed to groundwater. An alpha particle emitted near the

surface can emerge from the waste form and cause radiolysis of water if present.

The alpha particle dose model gets the alpha particle generation rate from the radiation source model. The model then updates a cumulative time integral of this alpha particle generation rate. The starting time for the integration is an input to the model. The conversion from number of alpha particles to atomic displacements, saturation factors, and any impact on waste form alteration will be part of the waste form alteration model and will be deferred to a future program version.

Alpha particles emitted from near the surface and in the right directions will exit from the waste form. We consider one average alpha particle energy; we then have one alpha particle range in the waste form solid. Alpha particle paths from a depth less than the range (taking angle of emission into account) will exit the waste form. For a generation rate  $C$  [particles/( $\text{sec} \times \text{m}^3$ )] and an energy  $E$  (MeV) corresponding to a range  $R$  (m), the number per second exiting the waste form is

$$CR/4 \text{ [number}/(\text{sec} \times \text{m}^2)\text{].}$$

These exiting alpha particles have a remaining energy averaging about  $E/2$  MeV, so the energy deposition rate in a water layer at the surface is

$$CRE/8 \text{ [(number} \times \text{MeV)} / (\text{sec} \times \text{m}^2)\text{].}$$

Part of this energy is converted into atomic ionizations. This absorbed energy is localized in a thin layer of the water volume. Any radiolysis products may diffuse into the larger water volume, or they may interact with the solid surface. The net effects of alpha dose rate on waste form alteration rate should be studied experimentally. The effect of the deposited energy on waste form alteration will be delegated to the waste form alteration model.

In summary, the outputs of the alpha particle dose model are:

- Alpha particle generation rate [number/( $\text{sec} \times \text{m}^3$  of waste form volume)].
- Cumulative alpha particle generation (number/ $\text{m}^3$  of waste form volume).
- Alpha particle absorbed dose rate at surface (number  $\times$  MeV)/( $\text{sec} \times \text{m}^2$  of waste form surface).

### 3.2.4 Spontaneous Fission and Neutron Dose Model

Spontaneous fissions produce two fission products which cause atomic displacement defects, as do alpha

particles. The fission product ranges are shorter and the energy deposition higher (both per-unit length and in total) than is the case for alpha particles from the alpha decay process. Associated with each fission a number of gamma rays and neutrons are generated; the average numbers per spontaneous fission are basic nuclear measurement data.

The fission dose model functions similarly to the alpha particle dose model. The dose rate and the dose in units of number/m<sup>3</sup> are calculated. Effects on the waste form will be deferred to a future program version and will be placed in the waste form alteration model.

### 3.3 Thermal Model

The thermal model calculates the temperature as a function of radial position in the waste package. The model assumes steady-state radial heat transfer. The inputs required are the heat generation rate of the waste form and the boundary temperature at the waste package/borehole wall interface, both as functions of time. This boundary temperature is provided by a more detailed model that handles non-steady-state conditions and the three-dimensional geometry of the waste containers and repository configuration (Stein et al., 1984; Burns, 1982).

The simplified thermal model has several uses:

- **Bookkeeping.** It can reconstruct the interior temperatures, while the data base from the detailed model needs to preserve only the boundary temperature history.
- **Sensitivity.** It can compare limited variations in waste package design, wherein heat generation is not altered but heat transfer is altered (e.g., by different thicknesses of air gaps).
- **Importance.** It can identify which waste package layers provide the largest temperature rises and which heat transfer processes are most effective in any layer.

The thermal model results are used as inputs to the mechanical, corrosion, waste package environment, waste form alteration, and waste transport models.

The steady-state assumption means we are neglecting the heat capacity of the waste package. This is important only during the early years after emplacement. WAPPA's thermal model is similar to ours in its assumption of steady state. The two-dimensional transient model TAC02D (Burns, 1982) was compared with WAPPA (Hockman and O'Neal, 1984). WAPPA's results were higher by as much as 7% (based on rise above ambient temperature). This difference occurred only at early times near the time of

peak temperature and at the center of the waste package. At later times a larger volume of the rock mass around the waste package is affected by the heat transfer, and the temperature field changes slowly. Then the thermal capacity of the rock mass acquires much greater importance than that of the waste package.

Therefore, one off-line calculation of the boundary temperature history serves for a range of waste package designs that have the same heat generation time history but differing arrangements or barrier materials. But if the waste package's heat generation history is scaled upward (e.g., by including more waste per package), then the boundary temperature history increases by more than linear proportion because the rock heat capacity remains a constant.

The thermal model assumes cylindrical symmetry and homogeneous material within an annulus. If the waste package design departs from this (e.g., with heat-transferring fins or locally inhomogeneous material), then the thermal model approach relies on an off-line 2-D or 3-D model to calculate the thermal field. The input thermal conductivity of the thermal model must then be adjusted to reproduce the temperature increase. That is, the thermal model's temperature increase across an annulus should match the actual temperature increase from the outside of the annulus to the hottest spot in the annulus.

With the steady-state model, the temperature gradient at each radius  $r$  is just that needed to transfer outward all the heat generated interior to that radius. Given the outer boundary temperature, the model calculates temperature increases from the outside inward, one annulus at a time. The model has formulas for solid annuli and for gas- and liquid-filled annuli. A solid annulus may be a heat source; this allows for several concentric waste forms in a single package. A gas-filled annulus can transfer heat by conduction, convection, and blackbody radiation. A liquid-filled annulus, if any, can transfer heat by conduction and convection.

Our thermal model approach is the same as WAPPA's, with some additions. We have added an equation for a hollow-annulus waste form. We have added convective heat transfer for a horizontally emplaced waste package; this is different from the convective heat transfer in the vertical case. We have added a check so that the ratio ( $k_e/k$ ) is never less than one (see Eq. 3.3-6).

The increases in temperature, proceeding from the waste package boundary inward, are calculated as follows.

The model first calculates for each annulus the heat generation per unit length (along the axis of the waste package).

$$Q_i \frac{(\text{Watts})}{(\text{m})} = q_i \frac{(\text{Watts})}{(\text{m}^3)} \times \pi (b^2 - a^2) \quad (3.3-1)$$

where

$q_i$  = provided by the radiation model

$i$  = the index number of the annulus

$b$  = outer radius (m)

$a$  = inner radius (m).

Starting from the outer annulus, the model calculates  $\Delta T$  across each annulus:

$$(T_i - T_o) = \Delta T = \Delta T_1 + \Delta T_2. \quad (3.3-2)$$

$\Delta T_1$  depends on the heat rate  $Q = \sum_j Q_j$  for annuli  $j$  interior to that annulus  $i$ .  $\Delta T_2$  depends on the heat rate in that annulus alone. Only an annulus with  $a > 0$  has some  $\Delta T_1$ . Only an annulus of solid material may be a waste form and have a nonzero  $\Delta T_2$ .

For an annulus of solid material,  $\Delta T_1$  is due to conduction only:

$$\Delta T_1 = \frac{Q}{2\pi k} \ln(b/a) \quad (3.3-3)$$

where

$k$  = thermal conductivity (W/m °C).

for

$$N_{Gr} < 2,000 \quad \frac{k_e}{k} = 1.0 \quad (3.3-5)$$

$$2,000 \leq N_{Gr} \leq 20,000 \quad \frac{k_e}{k} = 0.18(N_{Pr}/0.72)^{1/4} (N_{Gr})^{1/4} \left(\frac{l}{x}\right)^{-1/9} \quad (3.3-6)$$

$$20,000 \leq N_{Gr} \leq 11,000,000 \quad \frac{k_e}{k} = 0.065(N_{Pr}/0.72)^{1/3} (N_{Gr})^{1/3} \left(\frac{l}{x}\right)^{-1/9} \quad (3.3-7)$$

where

$x$  = radial gap distance (m)

$l$  = active length of the waste form (m);

but with a lower bound  $k_e/k = 1$ .

The correlations were based on measurements over a range where  $(l/x)$  did not exceed about 40. Our values may exceed this. The continuation of the correlation into this range is not assured. The ratio  $(k_e/k)$  will surely not be less than one; for large  $(l/x)$  values, we must explicitly check and reset  $(k_e/k)$  to be no less than one.

For a gas- or liquid-filled annulus, the conductive heat transfer is augmented by convective heat transfer. The same formula is used but with an effective thermal conductivity  $k_e$ , which includes natural convection effects as well as conduction. Empirical correlations of total heat transfer with relevant parameters have been developed, including the convection effects. We use correlations from Jacob (1949; pp. 534-542).

First,

$N_{Gr} \equiv$  Grashof Number (ratio of buoyancy forces to viscous forces in a free-convection flow system)

$$N_{Gr} = \frac{x^3 \rho^2 g \beta_f \Delta T}{\mu^2} \quad (3.3-4)$$

where

$x$  = gap dimension (m) =  $(b - a)$

$\rho$  = mean density of gas or liquid (kg/m<sup>3</sup>)

$g$  = acceleration due to gravity (m sec<sup>-2</sup>)

$\beta_f$  = volume expansion coefficient (°C<sup>-1</sup>)

$\Delta T$  = temperature difference across gap (°C)

$\mu$  = viscosity (kg m<sup>-1</sup>sec<sup>-1</sup>).

For a vertically emplaced cylindrical waste package, the correlations for  $k_e$  are:

For a horizontally emplaced, cylindrically symmetric waste package with a fluid annulus, for  $(b/a) \leq 2$  Jacob's correlations (1949) are:

for

$$N_{Gr} N_{Pr} < 1,000 \quad \frac{k_e}{k} = 1 \quad (3.3-8)$$

$$6,000 \leq N_{Gr} N_{Pr} \leq 10^6 \quad \frac{k_e}{k} = 0.11(N_{Gr} N_{Pr})^{0.29}$$

$$1 \leq N_{Pr} \leq 5,000 \quad (3.3-9)$$

$$10^6 \leq N_{Gr} N_{Pr} \leq 10^8 \quad \frac{k_e}{k} = 0.40(N_{Gr} N_{Pr})^{0.20}$$

$$1 \leq N_{Pr} \leq 5,000 \quad (3.3-10)$$

where

$N_{Pr}$  = Prandtl number (ratio of kinematic viscosity to thermal diffusivity).

$N_{Pr}$  is a property of the fluid; it may depend on temperature (we will use average temperature). (Note:  $N_{Pr} = 0.72$  for air.) Jacob does not specify  $(k_e/k)$  for  $1,000 < N_{Gr} N_{Pr} < 6,000$ . Presumably a smooth connecting curve could be filled in. We will use simply:

for

$$N_{Gr} N_{Pr} < 6,000 \quad \frac{k_e}{k} = 1. \quad (3.3-11)$$

The above  $(k_e/k)$  values are always greater than or equal to one. The ratio is not continuous at the boundary of the first and second domains. A future model might make it continuous if it turns out to be important for sensitivity studies.

For a gas-filled annulus, radiative heat transfer can also contribute. The total heat transfer rate is:

$$Q = \frac{2\pi k_e}{\ln(b/a)} (T_i - T_o) + 2\pi a F_{io} \sigma (T_i^4 - T_o^4) \quad (3.3-12)$$

where

$\sigma$  = Boltzmann constant ( $W/m^2K^4$ ).

$F_{io}$  is the radiative view factor from the inner to the outer wall (Jacob, 1957; Holman, 1981):

$$F_{io} = \frac{1}{\left(\frac{1}{\epsilon_i}\right) + \frac{a}{b} \left(\frac{1}{\epsilon_o} - 1\right)} \quad (3.3-13)$$

where

$\epsilon_i$  = hemispherical emittance of inner wall  
 $\epsilon_o$  = hemispherical emittance of outer wall.

The emittances are always less than one, so the denominator of  $F_{io}$  is always positive. In  $(T_i^4 - T_o^4)$ , the temperatures must be absolute ( $^{\circ}K$ ). In the linear

difference  $(T_i - T_o)$  the temperatures could be in  $^{\circ}K$  or  $^{\circ}C$  for the same result. The term  $(T_i^4 - T_o^4)$  may be factored:

$$(T_i^4 - T_o^4) = (T_i^3 + T_i^2 T_o + T_i T_o^2 + T_o^3)(T_i - T_o) \quad (3.3-14)$$

to give an all-positive-terms factor and a linear difference factor.

$k_e$  depends on  $N_{Gr}$  which depends on  $(T_i - T_o)$ . So in Eq. (3.3-12), both terms are nonlinear in  $(T_i - T_o)$ . Some of the parameters also depend on the average temperature in the annulus. Given  $Q$  and  $T_o$ , Eq. (3.3-12) will be solved for  $(T_i - T_o)$  or equivalently for  $T_i$ .

A solid annulus may have a nonzero  $\Delta T_2$  in Eq. (3.3-2) if it is a heat source. If so, then the same principle but different formulas apply for the two cases of inner radius zero and inner radius greater than zero. The principle is that the thermal gradient of  $T_2$  at  $r$  is sufficient to transfer the heat generated in that annulus interior to  $r$  (see Fig. 3-4). For derivation of thermally induced mechanical loads in solid annuli (Sec. 3.4) we will need not only  $\Delta T$  but also the temperature distribution for all radii  $r$  between  $a$  and  $b$ . As in Eq. (3.3-2), we distinguish two heat source locations and two terms in the temperature rise:

$$T(r) - T(b) = \Delta T(r) = \Delta T_1(r) + \Delta T_2(r) \quad (3.3-15)$$

for  $a \leq r \leq b$ .

For  $a > 0$  the combined effect from the two heat sources is:

$$\Delta T(r) = \frac{q}{4k} (b^2 - r^2) + \frac{1}{2\pi k} (Q - q\pi a^2) \ln\left(\frac{b}{r}\right) \quad (3.3-16)$$

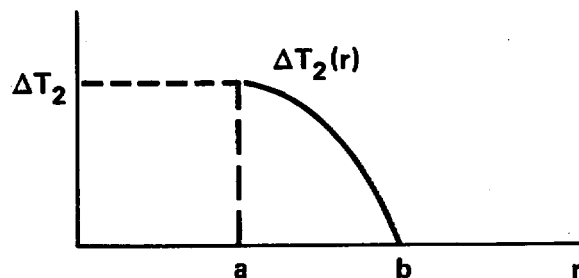


Figure 3-4. Temperature profile of  $T_2$  to transfer heat generated in an annulus. Not shown is  $T_1$  (the total temperature is  $T = T_1 + T_2$ ). The gradients of  $T_1$  and  $T_2$  are additive. The gradient of  $T_1$  transfers heat generated in interior annuli.

Recall that  $Q$  is the heat generation (per unit length along the waste package axis) interior to the annulus; and  $q$  is the heat generation per unit volume in that annulus.

For  $a = 0$  there is no further annulus interior to the current solid annulus, hence no  $Q$ . The result is:

$$\Delta T(r) = \frac{q}{4k} (b^2 - r^2). \quad (3.3-17)$$

### 3.4 Mechanical Model

The mechanical model calculates the mechanical stress at various locations in the waste package, checks for mechanical failure modes, and determines the revised mechanical condition of the waste package in case of a failure mode. The mechanical loads considered are listed in Table 3-2. Some mechanical loads not included in Table 3-2 are listed in Table 3-3; we will evaluate these in the future. The waste package's mechanical element types are listed in Table 3-4. The locations for stress evaluations and failure checks are the outer and inner surfaces of the waste package elements. (Even for yielding, the critical location seems to be the outer surface; nonetheless, we will check the inner surface as well.) We used the mechanical model in WAPPA, with some refinements. We note these differences after we describe the model.

The surface stress from the mechanical model will be used as input to the corrosion model. The waste form mechanical integrity condition will be used as input to the waste form release model. Changes in barrier integrity may also affect the thermal behavior and, thus, will be used as input for the thermal model.

We expect fairly low mechanical stresses for the reference design and its emplacement environment.

**Table 3-2. Loads included in the mechanical model.**

---

**External pressure**

- radial
- axial

**Constrained-displacement loads**

- thermal expansion
- corrosion products volume expansion

**Thermal gradient**

**Residual stress at closure weld**

**Arbitrary user-mandated failure (for "what-if" investigations)**

---

**Table 3-3. Mechanical topics deferred for future consideration.**

---

**Loads**

- weight of fallen roof rock blocks on the package
- gas and steam pressure inside the container
- individual fuel rod stresses

Alternate forms for stress intensity at a crack tip, as appropriate for the materials considered

---

**Table 3-4. Mechanical element types.**

---

Solid elastic element (e.g., glass waste form)

Cylindrical annulus, solid, elastic/plastic (e.g., metal barrier)

Cylindrical annulus, solid, incompressible, no strength in tension (e.g., a solid corrosion layer)

Fluid element

---

We include the mechanical model to verify this expectation and to handle "what-if" cases and variations on design. The residual stress at the closure weld may be the most important mechanical feature for waste package containment failure. A glass-pour waste canister may have a fairly large "shrink-fit" stress because of the different thermal expansion coefficients for glass and stainless steel. This is not a major issue for containment, however, because the canister will be enclosed in a second metal container to provide a well-controlled primary barrier.

The external pressure load could be hydrostatic or lithostatic. None is expected in the NNWSI repository, but a pressure load would be expected in a repository situated below the water table or in salt. An axial pressure would apply only to a borehole liner, if any, and to the outermost sealed container.

A constrained displacement load arises when a natural tendency of a material to expand or contract is constrained by the presence of a neighboring material. Two types of natural expansion are considered. The first is thermal expansion of a material at an increased or decreased average temperature. The second is the change in volume between a metal and the corresponding amount of corrosion product. We also include ductile yielding of a metal barrier, which could result in contact of two solid elements.

A thermal gradient in a solid element (in our case a gradient in the radial direction in a cylindrical annulus) generates a stress because of differential thermal expansion. The hotter side tends to expand, and the

cooler side tends to contract; however, the expansion and contraction are constrained by the solid structure of the element.

The closure weld of the primary container will have some residual stress in the weld and the heat-affected zone. (Other fabrication welds can be heat treated to relieve weld residual stress.) This stress will be variable along a weld and between packages. We will use the peak value in a package and treat it as a local stress to be added to the stress at the package surface (if the latter stress is tensile) when evaluating failure modes. The value to use will not be readily determinable; we will need to develop a distribution of values or estimated upper bounds.

An arbitrary user-mandated failure of any barrier is included. This will allow "what-if" studies of the exposure of the waste form to the local environment starting at a specified time. The input is simply the time of crack rupture failure or time of barrier thinning to zero.

Some loads will be evaluated in the future for possible inclusion in the model: (1) in the horizontal emplacement mode for a waste package, if some rock fragments or blocks come loose and rest on the package, the resulting stress will be tensile at certain areas on the circumference of the waste package. (2) A few fuel rods could have pinhole penetrations and be filled with water from the reactor; when heated the steam could leak into the spent fuel container and exert an interior pressure. (3) Individual fuel rods can have stresses due to their internal components. We neglect this for now and concentrate on the stresses in the principal barrier elements. (4) Inter-rod forces could arise if the fuel rods are not loosely packed.

The element types are listed in Table 3-4. The principal elements are waste forms and metal barriers. Other element types account for corrosion and gaps.

A glass waste form is considered to be elastic. It has a tensile yield stress for fracture formation at its surface. It has essentially no upper bound on compressive strength, because it is confined.

A spent fuel waste form is considered to be loosely packed and, hence, to have no stresses between fuel rods. To get this zero-stress effect we treat the waste form as an elastic solid with zero Young's modulus and bulk modulus.

A metal barrier is an elastic/plastic solid. It is subject to ductile movement when its yield stress is exceeded. It may fail by a rapidly propagating rupture of an existing crack. (Discussion of failure by stress corrosion cracking will be deferred till Sec. 3.6 on the corrosion model.)

A solid corrosion layer is allowed to transmit a compressive force between adjacent elements, but this layer has no tensile or shear strength.

A fluid element (liquid or gas) transmits no force. If a gas element is reduced to zero thickness by the movement of adjacent layers, we remove it temporarily from the stress calculation, thereby assuming there is enough volume at the ends of the waste package to accept the displaced gas without a major change in gas pressure.

The only force between two adjacent elements is a contact pressure. If a gap opens up between two solid elements—say due to different thermal expansion—then a gas gap is placed there in the model and the contact pressure is zero.

Thus, the possible forces on a single element are: (1) pressures on its interior and exterior surfaces and (2) forces due to a temperature gradient in the element. A series of solid elements in contact with one another will have displacement and pressure equalities at each interface. This leads to a matrix equation for the pressures. Solving that equation, we can then evaluate the interface displacements and the stresses.

The stresses and displacements in a single solid element, either an annulus or a central cylinder, are as follows. We assume the elements are free to expand in the axial direction. Thus we have a plane strain condition; i.e., axial strain is uniform over a plane perpendicular to the axial direction.

We separate the contributions to stresses  $\sigma$  and radial displacement  $u$  arising from (1) radial pressures on the two surfaces, (2) axial pressure, and (3) thermal effects:

$$\sigma_r = \sigma_r^P + \sigma_r^A + \sigma_r^T \quad (3.4-1)$$

$$\sigma_\theta = \sigma_\theta^P + \sigma_\theta^A + \sigma_\theta^T \quad (3.4-2)$$

$$\sigma_z = \sigma_z^P + \sigma_z^A + \sigma_z^T \quad (3.4-3)$$

$$u = u^P + u^A + u^T \quad (3.4-4)$$

where the subscripts  $r$ ,  $\theta$ , and  $z$  represent the cylindrical coordinates and the superscripts P, A, and T denote that the stress or displacement arises from inner and outer surface pressures, axial pressure, and thermal effects, respectively. Because of the cylindrical symmetry,  $\sigma$  and  $u$  are functions of  $r$  but not of  $\theta$  or  $z$ .

The axial pressure  $P_A$  affects only  $\sigma_z$  and  $u$ :

$$\sigma_r^A = 0 \quad (3.4-5)$$

$$\sigma_{\theta}^A = 0 \quad (3.4-6)$$

$$\sigma_z^A = -P_A \quad (3.4-7)$$

$$u^A = -\frac{r}{E} \nu \sigma_z^A = \frac{r}{E} \nu P_A \quad (3.4-8)$$

where

$E$  = Young's modulus (N/m<sup>2</sup>)

$\nu$  = Poisson's ratio (dimensionless).

Next, we discuss the stresses and displacement from the pressures  $P_i$  and  $P_o$  on the inner and outer interfaces (Wang, 1953, p. 56).

For a solid cylinder ( $a = 0$ )

$$\sigma_r^P = -P_o \quad (3.4-9)$$

$$\sigma_{\theta}^P = -P_o \quad (3.4-10)$$

$$\sigma_z^P = 0 \quad (3.4-11)$$

$$u^P = \frac{r}{E} (\sigma_{\theta}^P - \nu \sigma_r^P) = -\frac{r}{E} (1 - \nu) P_o \quad (3.4-12)$$

For an annulus ( $a > 0$  and  $a \leq r \leq b$ ):

$$\sigma_r^P = \frac{1}{b^2 - a^2} \left[ \frac{b^2(a^2 - r^2)}{r^2} P_o - \frac{a^2(b^2 - r^2)}{r^2} P_i \right] \quad (3.4-13)$$

$$\sigma_{\theta}^P = \frac{1}{b^2 - a^2} \left[ -\frac{b^2(a^2 - r^2)}{r^2} P_o + \frac{a^2(b^2 + r^2)}{r^2} P_i \right] \quad (3.4-14)$$

$$\sigma_z^P = 0 \quad (3.4-15)$$

$$u^P = \frac{r}{E} (\sigma_{\theta}^P - \nu \sigma_r^P) \quad (3.4-16)$$

We now discuss the thermal effects. See Wang (1953, p. 74) or Zudans et al. (1965, p. 232). To make the development as simple as possible and to be explicit about reference temperatures, we consider the element's temperature field to be the net result of two steps:

1. A uniform change from  $T_{ref}$  (the reference temperature at which thermal expansion from the reference dimensions is zero) to a uniform average temperature  $\bar{T}$ . This is accompanied by a uniform and unconstrained thermal expansion. There is no stress from this. The radial displacement from this is

$$u^u(r) = r \alpha (T - T_{ref}) \quad (3.4-17)$$

where  $\alpha$  = coefficient of thermal expansion ( $^{\circ}\text{C}^{-1}$  or  $^{\circ}\text{K}^{-1}$ ) and the superscript "u" indicates "unconstrained."

2. A change from  $\bar{T}$  to  $T(r)$ . The change is

$$T'(r) = T(r) - \bar{T}$$

This gives rise to thermal gradient stresses and an additional displacement  $u'(r)$ , but to no additional axial strain [ $\epsilon'_z(r) = 0$ ; we still have a plane strain condition].

For an annulus,

$$\sigma_r^T = -\frac{E\alpha}{1-\nu} \cdot \frac{1}{r^2} \int_a^r T' r' dr' \quad (3.4-18)$$

$$\sigma_{\theta}^T = \frac{E\alpha}{1-\nu} \left[ \frac{1}{r^2} \int_a^r T' r' dr' - T' \right] \quad (3.4-19)$$

$$\sigma_z^T = -\frac{E\alpha}{1-\nu} T' \quad (3.4-20)$$

$$u' = \frac{r}{E} \left[ \sigma_{\theta}^T - \nu (\sigma_r^T + \sigma_z^T) \right] + r \alpha T' \quad (3.4-21)$$

$$u' = \frac{1+\nu}{1-\nu} \frac{\alpha}{r} \int_a^r T' r' dr' \quad (3.4-22)$$

Note that these stress equations satisfy the plane-strain condition with  $\epsilon'_z = 0$ :

$$\sigma_z^T = \nu (\sigma_r^T + \sigma_{\theta}^T) - E\alpha T' \quad (3.4-23)$$

There is also an algebraic equality:

$$\sigma_{\theta}^T = \sigma_z^T - \sigma_r^T \quad (3.4-24)$$

The stresses and displacement given by Eqs. (3.4-18) through (3.4-22) depend on an area-weighted integral of  $T'$  between  $a$  and  $r$ :

$$\int_a^r T' r' dr' \quad (3.4-25)$$

This integral equals zero when  $r = b$ . If  $a > 0$ , we can evaluate the case  $r = a$  directly. The integral equals zero in this case also.

For a central cylinder ( $a = 0$ ) the same equations apply, but we must evaluate the stress values for  $r = 0$  as a limit. As  $r$  approaches zero, the stresses and displacements approach their values for  $r = 0$ :

$$\sigma_r^T(0) = -\frac{E\alpha}{2(1-\nu)} T'(0) \quad (3.4-26)$$

$$\sigma_\theta^T(0) = -\frac{E\alpha}{2(1-\nu)} T'(0) \quad (3.4-27)$$

$$\sigma_z^T(0) = -\frac{E\alpha}{(1-\nu)} T'(0) \quad (3.4-28)$$

$$u'(0) = 0 \quad (3.4-29)$$

An annulus and a central cylinder have temperature fields  $T(r)$  of somewhat different algebraic form; see Eqs. (3.3-16) and (3.3-17). Then the averages  $\bar{T}$ , the differences  $T'$  from the averages, and the averages of  $T'$  between  $a$  and  $r$  will be somewhat different. The equations for these are straightforward but in some cases lengthy. That is:

$$T(r) = T_0 + \Delta T(r) \quad (3.4-30)$$

where  $\Delta T(r)$  is from Eqs. (3.3-16) or (3.3-17).

$$T = T_0 + \overline{\Delta T(r)} \quad (3.4-31)$$

$$T'(r) = \Delta T(r) - \overline{\Delta T(r)} \quad (3.4-32)$$

We are expressing  $T'(r)$  and  $\Delta T(r)$  as a function of  $Q$  and/or  $q$ . We could equivalently express it in terms of the total  $\Delta T = \Delta T(a)$  as does WAPPA. But because Eq. (3.3-16) has two terms,  $Q$  and  $q$  would not be eliminated. To find  $\overline{\Delta T(r)}$  and then to evaluate the integrals in Eqs. (3.4-18) through (3.4-22), we need to evaluate the integrals:

$$\int_a^r r' dr'$$

$$\int_a^r r'^3 dr'$$

$$\int_a^r (\ln r') r' dr'$$

where  $r$  is some intermediate value or the upper-limit value  $b$ , and in the first two integrals  $a$  may be zero. These integrals have relatively simple algebraic forms. The rest is substitution, which may be done by a sequence of algebraic steps or a corresponding sequence of lines in a FORTRAN computer code.

The total thermal displacement is

$$u^T = u^u + u' \quad (3.4-33)$$

with  $u^u$  and  $u'$  from Eqs. (3.4-17) and (3.4-22).

For total displacement we may also write

$$u = -(\sigma_\theta - \nu(\sigma_r + \sigma_z)) + r\alpha(T - T_{ref}) \quad (3.4-34)$$

However, the algebraic form based on Eq. (3.4-4) with Eqs. (3.4-8), (3.4-16), and (3.4-33) is the appropriate one to use in setting up the multiple annulus contact problem, since only  $u^p$  depends on  $P_i$  and  $P_o$ . Solution of a matrix equation leads to the interface displacements, pressures, and then the stresses at any surface or interior location.

With the imposed stresses, the metal barrier annuli are subject to ductile yielding. The maximum shear stress theory or Tresca criterion (Mendelson, 1968, p. 73) is used for the threshold for yielding:

$$\text{Max}(|\sigma_r - \sigma_\theta|, |\sigma_\theta - \sigma_z|, |\sigma_z - \sigma_r|) = \sigma_{\text{yield}} \quad (3.4-35)$$

When this threshold is reached, the material can still support differences in principal stress equal to  $\sigma_{\text{yield}}$ . The material deforms until a new geometry with static balance of forces is attained. Cylindrical symmetry is maintained. This maintenance of symmetry is an uncertain assumption unless the yielding displacement is very small. Hence, cases with yielding will be flagged for further inspection outside the PANDORA program.

The metal barrier annuli are subject to crack rupture. Provisionally, we use the approach that rupture

occurs and propagates if the stress intensity at the tip of a preexisting crack exceeds a threshold value, which may depend on temperature. The stress intensity is calculated by:

$$k_1 = C\sigma\sqrt{\pi a_c} \quad (3.4-36)$$

where

- $k_1$  = stress intensity ( $N/m^{3/2}$ )
- $\sigma$  = principal stress component, axial or circumferential ( $N/m^2$ )
- $a_c$  = crack size (m)
- $C$  is a constant:
- $C = 2.24/\pi$  if  $a_c <$  barrier thickness
- $C = 1$  if  $a_c >$  barrier thickness.

In future work, we will gather data for initiation of crack rupture for the metals proposed for the waste package. This data may include enabling conditions, threshold values, and the form of the threshold equation to substitute for Eq. (3.4-36). Generally, we expect modification of Eq. (3.4-36) for metals with large ductility: i.e., large ratios of rupture strain to yield strain.

Our mechanical model is essentially the same as WAPPA's with the following exceptions:

1. WAPPA's  $T_{ref}$  is zero degrees, since it does not appear explicitly. Our  $T_{ref}$  is user-input and may be different for each element.
2. WAPPA's external axial pressure applies to all elements. In our model, it only applies to the outermost sealed barrier.
3. We put in or take out an air gap as appropriate. WAPPA's air gaps are user-specified and are permanent, transmitting no pressure, even if their gap thickness vanishes or becomes negative.
4. Our temperature field for an annulus [Eq. (3.3-16)] has an annulus heat source  $q$  as well as an interior heat  $Q$ . This extension leads to an extension in the thermal stress equations. The latter extension would only apply to an annular glass waste form because the spent fuel waste form is expected to be loosely packed.
5. We have added weld residual stress as a local stress.
6. WAPPA's Users Manual has a few typographical errors in the stress equations. We have tried to avoid errors by separating the equations into smaller pieces, by substituting new symbols for some repeated aggregates of symbols, and by cross checks such as verification of the plane strain condition.

### 3.5 Waste Package Environment Model

The waste package environment model evaluates the flow of water, steam, and air which can affect the waste package barriers and the waste form and can assist later in waste transport. The waste package environment model should describe how water will contact the package and later the waste form, and how much water volume per year will effectively contact the waste package or waste form. In the following discussion, after sketching what might happen, we describe a simple model which bounds the possible cases.

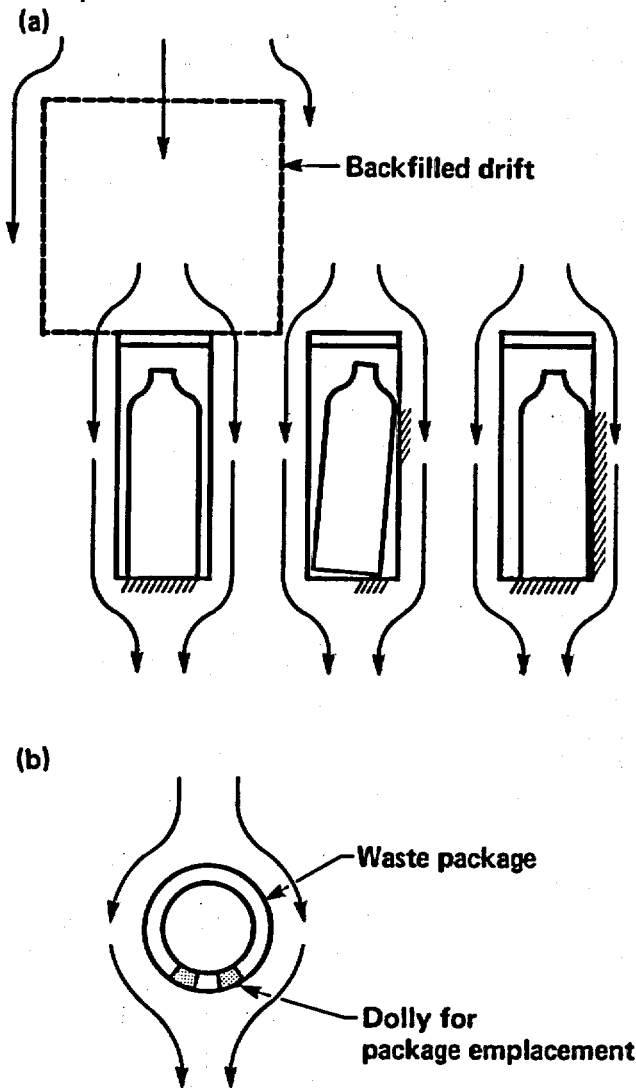
In the early years after emplacement when the package surface is above  $95^\circ C$ , the package will be in a steam/air environment. Some time after the temperature drops below  $95^\circ C$ , groundwater flow will be reestablished. After a transient period, the groundwater flow will approach a steady-state condition. We will use the program TOUGH (Pruess and Wang, 1984), or equivalent, to calculate both the rewetting time of the rock around the emplacement hole and the water flux in the transient period. On a repository-scale average, the steady-state water flux will be about what it was before the repository was established.

The steady-state water flux is downward by unsaturated flow in the porous rock. Any flow in fractures will tend to be absorbed into the porous rock matrix unless the flux exceeds a threshold value locally (one of our future data needs). The flow parameters at the proposed Yucca Mountain site are on the average a water flux of less than 0.2 mm/year, and a partial saturation of about 65% (Montazer and Wilson, 1984). A water flux value of 1 mm/year has been adopted for purposes of waste package design and testing (SCP, Sec. 7.1).

The likely flow at an emplacement hole is around the hole, keeping to the rock matrix, rather than into the hole (see Fig. 3-5). In such a flow regime, a waste package could be wetted only where it touches the rock.

For some emplacement holes, there is a possibility that local variations in rock permeability will divert water flow into fractures which intersect the hole. If that occurs, some water could drip into the hole and flow over the waste package (see Fig. 3-6).

The simplified model assumes that all the water flux passing through a certain area above the waste package will flow into the emplacement hole and contact the waste package. The specified area may be that extending to a distance of  $N$  times the emplacement hole radius. Because the water flux at the site is



Key:  
 //////////////// Contact with moist rock

Figure 3-5. The most common water flow pattern is expected to be around the emplacement boreholes and through the rock, rather than through the boreholes. The waste package will be in partial contact with the host rock, which will be moist after groundwater flow is reestablished. A horizontally emplaced waste package will not contact the rock until after the borehole liner (if used) and emplacement guide rails have corroded. (a) Vertical emplacement. (b) Horizontal emplacement.

so low, preliminary calculations indicate we could conservatively extend the distance out halfway to the neighboring emplacement holes without introducing any problems with waste package performance.

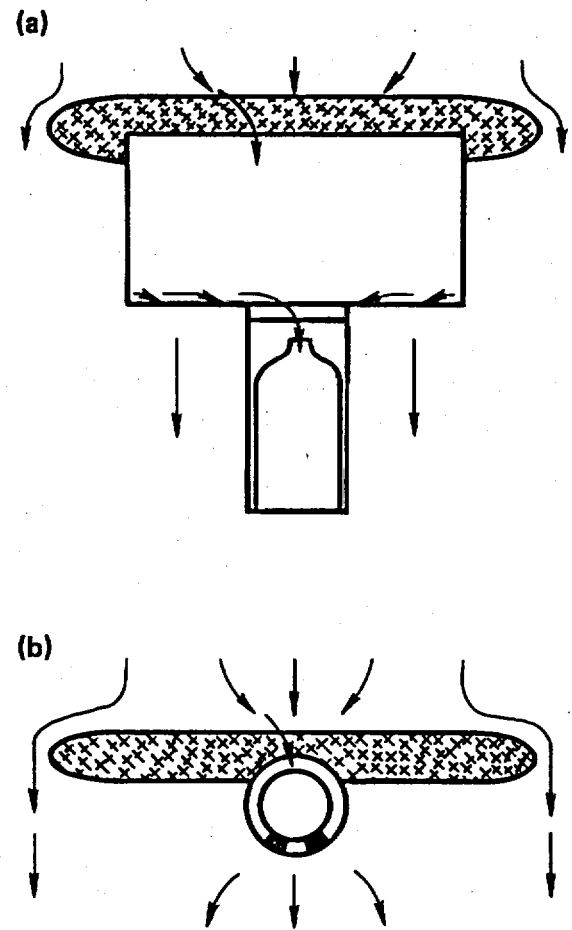


Figure 3-6. For some emplaced waste packages, it is possible that conditions differing from the average conditions will allow water to enter the emplacement borehole. A lens of rock with lower than average permeability could divert the groundwater flux to increase it in some areas. This local flux coupled with fracture permeability could introduce water dripping into the borehole. Our simplified modeling strategy is to assume that the water flux through a specified area somehow is led into the borehole.

After the water's influx to the emplacement hole, we simply assume that the water can keep part of the package wet; e.g., we look at general corrosion on a wetted surface rather than averaged over the full surface of the waste package.

The barrier element's containment function may eventually be lost as corrosion zones penetrate the barrier. One candidate area for the earliest penetrations is the final closure weld of the barrier element. In the vertical emplacement case, penetration in the closure weld will be near the top of the emplaced

package, allowing the package to retain standing water. In the horizontal emplacement case, weld corrosion in several spots could allow water to trickle through and drain out of the package. We model these alternatives with two models of water contact with the waste form, the bathtub model and the trickle model.

If there is a hole only near the top of the waste package we may have a bathtub or holding tank effect. After the tank is filled, an inflow of new water is balanced by an outflow of an equal amount of water containing dissolved waste. The water stays in contact with the waste form long enough to reach a steady state (e.g., steady-state concentrations of low solubility substances comprising the waste form). If there are also holes near the bottom of the container, we assume that water moves downward with limited contact time with the waste form, and then moves with the rapid transport of dissolved waste quantities to the boundary of the waste package.

With this model, we need not know any more details of the water's movement within the degraded waste package.

Specifically, the inputs required for the waste package environment model are:

1. Water flux (m/y) (volume of water per year per unit cross-sectional area in a horizontal plane above the waste package) as a function of time; after a certain time this becomes a steady-state value.

Note: The boundary condition of water flux as a function of time should be coordinated with the boundary condition of temperature as a function of time.

2. Surface area of the "catchment area" above the package, from which water flux will flow into the waste package emplacement hole (m<sup>2</sup>).

3. Void volume of waste package available for retention of standing water.

4. Water quality: dissolved chloride and silicon (as a mass fraction) of the water) as a function of time. (This feature is deferred to a future model version.)

The outputs as a function of time are:

1. Inflow rate (m<sup>3</sup>/y) of water flow per waste package.
2. Stored water volume in package (m<sup>3</sup>).
3. Average dissolved chloride and silicon (as a mass fraction) in the stored water (in a later version).
4. Outflow rate (m<sup>3</sup>/y).

### 3.6 Corrosion Model

The corrosion model calculates the thickness of material altered by oxidation or aqueous general corro-

sion. We are deferring to a future model the incorporation of checks for environmental conditions, which would allow other modes of corrosion, such as intergranular stress corrosion cracking, pitting, and crevice corrosion. Threshold conditions for these modes, or conservative envelopes on such thresholds, and the corrosion rates for the modes will be obtained by the corrosion testing program being conducted within the NNWSI Project using site-specific groundwater properties and environmental conditions.

Corrosion-induced changes in material thickness will affect the thermal and mechanical behavior. Changes in barrier integrity due to corrosion will affect thermal, mechanical, fluid flow, and waste form release behavior. Corrosion model output will be used as input to the corresponding models.

Corrosion modes and corrosion-enabling conditions are discussed in Sec. 7.4.2 of the SCP. General corrosion rates for the stainless steel containment barrier are sufficiently low that the container will remain substantially intact for more than 10,000 years. Therefore attention is directed to localized corrosion mechanisms, such as intergranular stress corrosion cracking and crevice corrosion, which, if they occur at all, would proceed more rapidly than general corrosion. The Metal Barriers subtask is investigating the mechanisms and conditions relevant to the occurrence of the corrosion modes and the corresponding precautions in metallurgy, fabrication, and environmental conditions needed to ensure that these modes are not enabled. In a future version, the PANDORA model can take conservative envelopes of the sensitizing and enabling conditions and can track the package parameters to check that the parameters stay on the safe side of the envelopes. The remaining concerns with localized corrosion modes seem to be variability in some conditions (such as the closure weld's residual stress) and scenarios that might produce off-normal environmental conditions at a few locations on a few of the waste packages. These are potential topics for a future probabilistic performance model.

The factors relevant to corrosion mode thresholds that can be tracked by the waste package system model, if required, include:

1. Environment type: air-steam, air-water vapor below the boiling temperature, water, or an alternation of water and moist air.
2. Temperature.
3. Gamma ray dose rate in water.
4. Tensile stress at metal barrier surface.
5. Chloride ion concentration in the ground water.

Some possible threshold factors (such as off-average solute concentrations in crevices at some locations)

may have to be input to the model rather than calculated within the model.

The first-generation corrosion model considers general corrosion in three environments:

- Air and steam.
- Air and water vapor.
- Water.

The model will look up the following in input data tables, as a function of temperature and gamma ray dose rate in water:

- Corrosion rate of the metal (m/y).
- Percentage of the corrosion product that remains on the surface as a solid layer.
- Rate of removal of an existing corrosion product layer by water (m/y).

Another input data item, required for transfer to the mechanical model, is the change in specific volume between the metal and the corresponding amount of solid corrosion product.

### 3.7 Waste Form Alteration Model

The waste form alteration model calculates the quantity per year released into mobile forms of each radionuclide and of the waste form matrix. The mobile forms are gases (noble gases and CO<sub>2</sub>) and solutes in water. The model and the input values are based on the work of the Waste Form Performance subtask within the NNWSI Project (SCP, Sec. 7.4.3).

The source term for spent fuel includes five components:

1. Radionuclides present in part in the oxidized layer on the outer surface of the Zircaloy fuel rod cladding and available for rapid release when the container is breached.
2. Radionuclides contained in the fuel rod cladding.
3. Radionuclides contained in stainless steel or Inconel fuel assembly components.
4. Radionuclides present in part in the fuel/cladding gap and available for rapid release when the cladding is breached.
5. Radionuclides whose release is controlled by the spent fuel pellet matrix dissolution rate.

Some of the radionuclides in the spent fuel matrix may be mobilized more slowly than the matrix because of their low solubility. In a solubility limit, both radioactive and stable isotopes of an element must be counted.

Given a container breach, the rapid-release fractions are spread over time because of the distribution of time-to-breach for containers and time-to-breach for cladding of fuel pins. The present PANDORA model

deals with a single container; the total release from a group of containers will be deferred to future work.

The units for mobilization rates and for inventories of radionuclides in a mobile form (but still within the waste package geometric boundary) are in terms of fraction of the inventory of a whole waste package at that current time. Thus radioactive decay and buildup can be accounted for simply by reference to the ORIGEN2 inventory tables.

The first radionuclide released will probably be carbon-14 from the outer oxidized layer of the cladding. Experiments conducted in air at a high temperature (275°C) have shown that there is an initial rapid release of about 0.25% of a fuel assembly's inventory of C-14 as CO<sub>2</sub> gas (Van Konynenburg et al., 1984). The fraction of prompt release is an input data element of the waste form mobilization model.

Cladding degradation has two functional effects. Cladding corrosion exposes activation products contained in the cladding material. Cladding breach initiates the exposure of the spent fuel within the fuel rod. An input to the model is the corrosion rate of the Zircaloy under site-specific conditions, in units of the fraction of the Zircaloy inventory of the waste package corroded per year. We assume that activation products contained in the cladding material are converted into mobile form congruent with the Zircaloy corrosion, except for zirconium, which is limited by its solubility.

Similarly, the corrosion of stainless steel and Inconel components exposes activation products contained in these materials. An input to the model is the corrosion rate of these materials under site-specific conditions, in units of the fraction of the inventory in the waste package corroded per year. We assume that activation products contained in the material are converted into mobile form congruent with the corrosion, except for nickel, which may be limited by its solubility if there is a large amount of stable nickel in the material.

For certain waste elements in spent fuel, there is a fraction of their inventory which, when exposed to water, is mobilized promptly or within a few years. The mobilization rates later settle down to be congruent with the mobilization rate of the waste form matrix. This fast-release fraction in spent fuel is due to materials segregated in the fuel-cladding gap or on the fuel grain boundaries; these materials can be dissolved when water penetrates the cladding. Some of this fraction may have come from leaching from the solid UO<sub>2</sub> either along fine cracks or along intergranular surfaces when the fuel was at reactor operating temperatures. The release of this fraction will slow down in time, due to depletion of the inventory in the gap and in grain boundaries near the fuel pellet surface.

The highest initial release rate is for cesium. A typical value for the fraction available for fast release is 0.5% of the cesium inventory. There is a lesser initial release rate for technetium (Oversby and Wilson, 1985). (Noble gases among the fission products would also have an initial release rate, but none of the noble gases are a significant part of the spent fuel radioactivity inventory at the end of the containment period. Krypton-85 has a half-life of 10.76 years.)

The later congruent release of radioactive atoms with release of the  $\text{UO}_2$  spent fuel matrix is not the only logical possibility, but it is observed in fact. Conceivably the  $\text{UO}_2$  could rearrange itself in crystal structure or reprecipitation faster than the net rate of removal in solution. This could expose the inner contents to liquid solution. Experimentally, however, the highly soluble elements such as technetium do settle down to a release rate into solution which is approximately congruent to the dissolution rate of uranium, i.e., in proportion to the ratio of technetium to uranium in the solid.

In the computer model, the fast-release fraction is handled by tables. For this fast-release process, we assume that the fraction of inventory released into water per year is the same as that observed in the measurements, despite the fact that a smaller volume of water per year is available in the planned waste package disposal location than in the measurements. We condense all of the fast-release fraction of a fuel rod, which may actually be released over several years, into the first year after the fuel rod cladding fails. (The distribution over time of cladding breach-times will spread the inventory release over time.)

The congruent release into water of the waste form matrix and contained elements does depend strongly on the water flux. We assume that matrix dissolution rate is the limiting factor for the contained elements' release rate. The matrix dissolution rate depends on the scenario for water flow in the waste package. If the barrier container has several perforations and the groundwater trickles through, then the matrix dissolution rate will be determined from measurements under similar conditions and comparable water flow rate. If the barrier container has one perforation placed so that water can fill up the container, then the spent fuel will eventually be exposed continuously to a nearly fixed mass of water. A small rate of inflow of new water will displace an equal amount from the standing water. In measurements with spent fuel in standing water (SCP, Sec. 7.4.3.2) the amount of uranium in solution eventually reached an apparent solubility limit for the uranium. In this case, the matrix dissolution rate is determined by the solubility together with the refresh water flow rate. In our model

for the standing water (bathtub) case, all the water flux through the emplacement hole contacts the waste form and departs carrying a solubility limit of uranium and a congruent amount of the other materials in the spent fuel. In a future model version, the amount of the other materials will be limited by their own solubility or congruent dissolution, whichever is less.

The waste form alteration model may require inputs from the fluid flow and thermal models. Since the temperature of liquid water has a limited range of  $95^\circ\text{C}$  and below, we may be able to use the waste matrix solubility at  $95^\circ\text{C}$  and neglect solubility decreases at lower temperatures. The waste matrix alpha particle dose history and the current radiation dose rate in water do not affect the present solubility-limited dissolution model, but may affect both the solubility and the rate of dissolution in a solubility-kinetics-limited model.

The waste form alteration model affects the waste package model in that it reduces the inventory of the waste form in the waste package. The waste form alteration model does not affect the radiation source model; the amount of material removed from the surface of the waste form does not affect the source because the waste form is a thick self-shielding source. There is a small effect on the gamma ray attenuation because some radiation source material is mobilized and transported beyond intervening barriers to a location where it can irradiate a barrier directly. We can neglect this effect because:

1. By the time the containment barrier has been breached, the gamma radiation source strength is very low.
2. The fraction of the waste mobilized but still within the waste form geometry is a very small fraction of the total.
3. The barriers are already breached, so corrosion and radiation effects on corrosion are no longer of leading importance.

The following notes complete the specification of our model:

1. For the matrix-limited component of waste release, we assume that this release begins at its full rate when the first fuel rod cladding is breached. This assumes that the release is limited by water flow and/or matrix solubility rather than the fraction of the fuel rods exposed to the water flow.
2. For a radionuclide with a fast-release fraction of  $X\%$ , we assume that the last  $X\%$  of the matrix has none of this nuclide, and the first  $(100 - X)\%$  has a concentration of this nuclide determined from the total inventory of the nuclide divided by the total inventory of uranium.

For a glass waste form, the waste form alteration model assumes that release of all elements is controlled by the matrix alteration rate. This rate will be input as determined for two water flow scenarios: the trickle-through scenario and the standing-water scenario. (In the standing-water scenario, the water container is more likely to be the outer primary barrier rather than the glass-pour container; the latter will probably be less durable because of its exposure to heat and stress during the glass pour and cooling operations.)

### 3.8 Waste Transport Model

The waste transport model calculates the flux of each radionuclide at the waste package/repository host rock interface. The interface is at the borehole wall. In a future version of the model, calculations will also be done at some distance into the rock.

The flux is in units of fraction per year of the current inventory of a whole waste package. The flux is also reported in units of grams per year and in units of the fraction per year of the inventory of a whole waste package at 1,000 years after removal from the reactor. The model requires as inputs the fluid flow results and the waste mobilization rate within the waste package volume.

For water soluble elements, we consider advection with the water flux. The model assumes that the water flux out equals the water flux in (after an initial fill time in the bathtub scenario). Elements dissolved in the standing water are transported out of the waste package volume with the outgoing water flux. The fast-release fractions of the waste will be spread out over time by the distributions of the time-to-failure of the waste containers and fuel rod cladding.

When a single container develops a second breach, its standing water and dissolved radionuclides could be released within one year. But for a group of containers, this release is spread out over time: first, by the distribution of time to first breach; and second, by the distribution of time to a second breach at a lower elevation, given a first breach.

For gases, transport is by diffusion into the host rock. We assume that any gases mobilized after the first breach are immediately available for transport beyond the boundary of the waste package.

### 3.9 Driver Model

The driver model couples all the process models, calculates the time history of the waste package's

condition and processes, and from this time history extracts the performance measures.

The specific solution is essentially determined by the initial conditions and the boundary conditions over time. Figure 3-7 shows the overall structure of operations establishing the initial and boundary conditions and calculating the waste package performance. We use Gane and Sarson's (1979) notation for data flow diagrams—see Fig. 3-8.

Data delivered to the process models must come from the proper sources and have the current-time values. Data flow diagrams show the logical dependencies of data needs but abstain from specifying program sequence or control. Data flow diagrams are a good starting point for the specification of the necessary properties of the linkages among the process models.

Our construction of the data flow diagrams for the driver model is presented in a sequence to express some of the time properties of the data and to clarify parts of the process being modeled. Some data adjust to the boundary conditions with essentially no time delay, e.g., radiation, temperature, and stress. Some data change slowly with time, e.g., intact barrier thickness as reduced by corrosion. Some data have discrete values and change infrequently but suddenly, e.g., barrier surface environment (dry/wet), barrier strength (intact/yielded), and barrier integrity (intact/breached).

Figure 3-9 and Table 3-5 show some data that adjust immediately to the boundary conditions; they also show the associated processes. The radiation model's heat source rate, radiation source rate, and attenuated gamma ray dose rate are immediately dependent on the input value from the radiation source time history. The temperatures adjust to the heat source rate and the input value from the boundary temperature time history. The mechanical stresses immediately find a static equilibrium dependent on the temperatures and the input value from the boundary pressure time history.

The environmental condition and the corrosion rates also depend on the current-time boundary conditions and on the data shown in Fig. 3-9; see Fig. 3-10 and Table 3-6. (An additional output from the environmental model has a time delay: this is introduced in Fig. 3-14.)

Some waste package data change slowly over time. For example, the geometry (intact barrier thicknesses) changes slowly due to general corrosion; see Fig. 3-11 and Table 3-7.

Now the sequence of diagramming has reached a closed feedback loop. The processes in the loop are shown in Fig. 3-12. (The external data stores of material properties and boundary time histories are not

drawn but are implied.) The progression of corrosion affects barrier thickness. The latter affects gamma ray attenuation and heat transfer, both of which affect corrosion rate. The corrosion rate affects the further progress of corrosion and of barrier thickness change.

Some waste package data have discrete values and change infrequently but suddenly. The progression of corrosion implies that eventually the barrier's containment integrity will be lost. Mechanical yielding or rupture occur rapidly when a threshold stress is

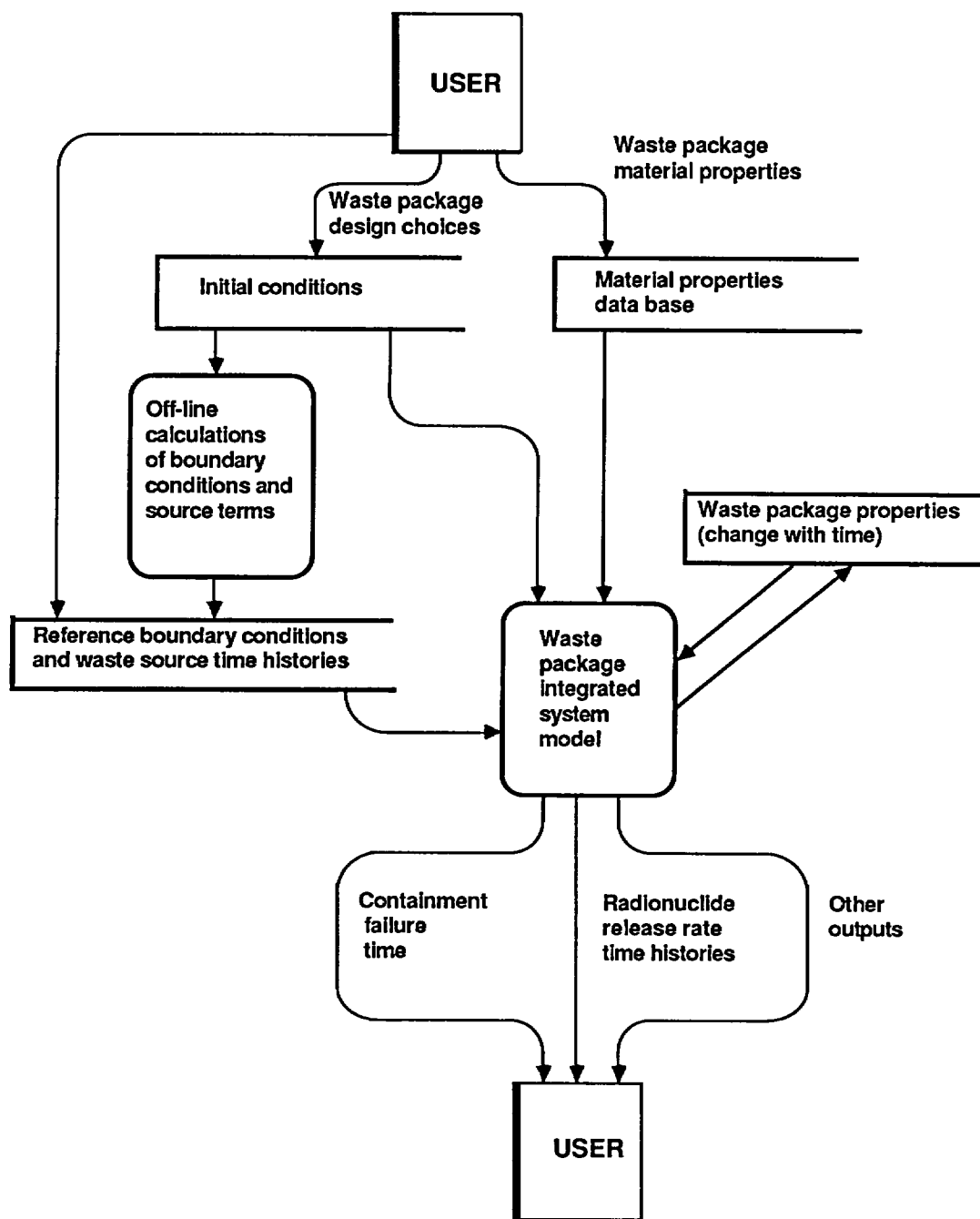


Figure 3-7. Data flows, data stores, and grouped inputs and outputs for the waste package system performance problem.

reached. Some modes of corrosion may occur and progress rapidly when enabling environmental and stress conditions are reached. A test for conditions for failure modes is included in Fig. 3-13; added data flows are described in Table 3-8. The failure modes process requires many of the same data required by the corrosion rate process. Data required from the general

corrosion increment process can be acquired through the waste package properties data store. The failure modes process requires the time value only to report the time if a failure does occur.

The waste form alteration and waste transport models depend on data developed by the other models, including additional data not required for the corrosion

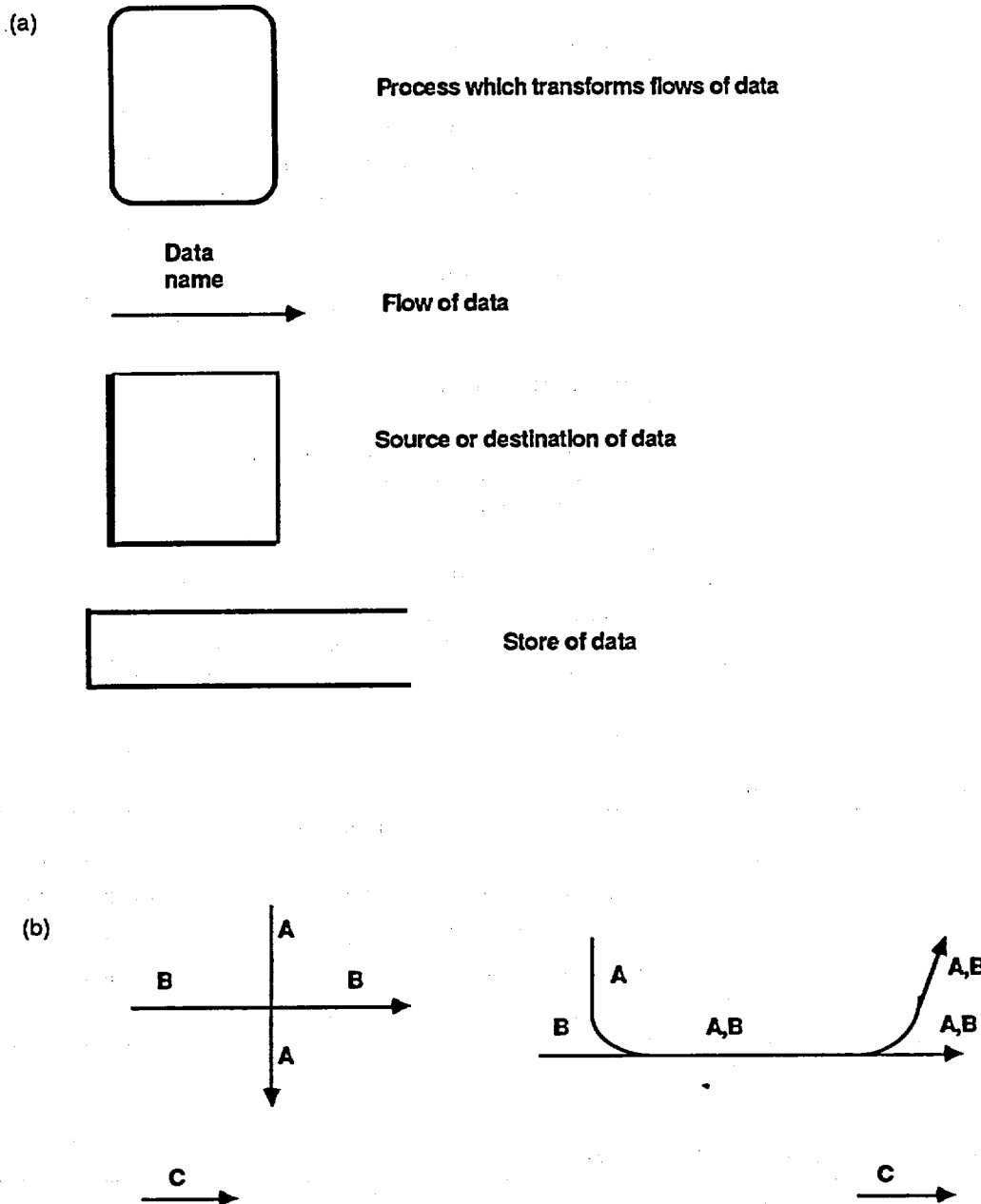


Figure 3-8. Data flow symbols and conventions. (a) Data flow symbols. (b) Conventions. Crossed data flow lines do not join; merging lines do join. To avoid "spaghetti diagrams," connectivity may be indicated by labeling with the data group name, or an entity such as a data store may be drawn in duplicate positions. A data flow indicates data needs and sources; it does not indicate sequence or control.

**Table 3-5. Elements of the data dictionary for Fig. 3-9.**

<b>Data label</b>	<b>Data contents</b>
<b>Waste package properties</b>	<b>Geometry</b> <b>Status of elements</b> <b>Environment (dry/wet)</b> <b>Strength (Intact/yielded)</b> <b>Integrity (intact/breached)</b> <b>Material types</b> <b>Quantity of waste form</b>
<b>G</b>	<b>Waste package geometry</b>
<b>S</b>	<b>Status of waste package elements</b>
<b>DB</b>	<b>Data base of material properties</b>
<b>Radiation source t/h</b>	<b>Time history of radionuclide inventories, heat generation rate, radiation generation rate</b>
<b>Boundary temp t/h</b>	<b>Time history of boundary temperature</b>
<b>Boundary pressure t/h</b>	<b>Time history of external pressures in axial and radial directions of waste package</b>
<b>time</b>	<b>Current time</b>
<b>Heat rate</b>	<b>Heat generation rate of each waste form</b>
<b>R1</b>	<b>Radiation data:</b> <b>Gamma ray absorbed dose rate in water at waste form surface and at surface of each barrier element</b>
<b>Temp</b>	<b>Temperature at inner and outer surfaces of each element of the waste package</b>
<b>Stress</b>	<b>Stress components at surfaces of each barrier element and at surface and interior of waste form</b>

**Table 3-6. Data dictionary elements added for Fig. 3-10.**

<b>Data label</b>	<b>Data contents</b>
<b>Boundary fluid flow t/h</b>	<b>Time history of rate of water flow into the waste package volume</b>
<b>Corrosion rate</b>	<b>General corrosion rate for each barrier</b>
<b>Wet(Y/N)</b>	<b>Wet (yes/no) environmental status of boundary of waste package</b>
<b>Water flow rate</b>	<b>Water flow rate into the waste package volume</b>

**Table 3-7. Data dictionary elements added for Fig. 3-11.**

<b>Data label</b>	<b>Data contents</b>
<b>Time</b>	<b>Current time, time of next time step</b>
<b>New thickness</b>	<b>New thickness of intact barriers and of corrosion layers</b>

model; see Fig. 3-14 and Table 3-9. These data include alpha particle and spontaneous fission doses and dose rates, radionuclide inventories per unit of waste form inventory, and quantity of water retained in a partially degraded waste package. Some of these data depend on past history as well as current conditions. The waste form alteration and waste transport models affect one item of the waste package data, the quantity of waste form. The driver model's solution method calculates the history of the waste package's condition and processes in the time domain, and from this time history extracts the performance measures. The algorithm uses large time intervals when conditions and package parameters are changing slowly, and short time intervals when conditions or parameters change with large rates or discretely. The algorithm calculates current-time conditions, then projects corrosion, waste form alteration, and waste release over an interval to the next time, and then calculates next-time conditions

and checks for discrete status changes or the exceedence of failure thresholds. If any such change is indicated, the algorithm returns to the current-time and repeats the projection with a smaller time step. If a discrete change occurs during a minimum time interval (specified by the user, down to a minimum of one year), then the waste package status is updated with the change at the current time. If no discrete change occurs during a time interval, then the continuous process results are updated and the next-time becomes the current-time for the start of the next step.

This algorithm models both discrete and continuous changes in waste package condition, identifies the time of loss of containment to within a desired tolerance, and provides radionuclide release rates and release quantities over a time interval. More details of implementation will be developed during the program design stage, but the final algorithm will perform functionally as described.

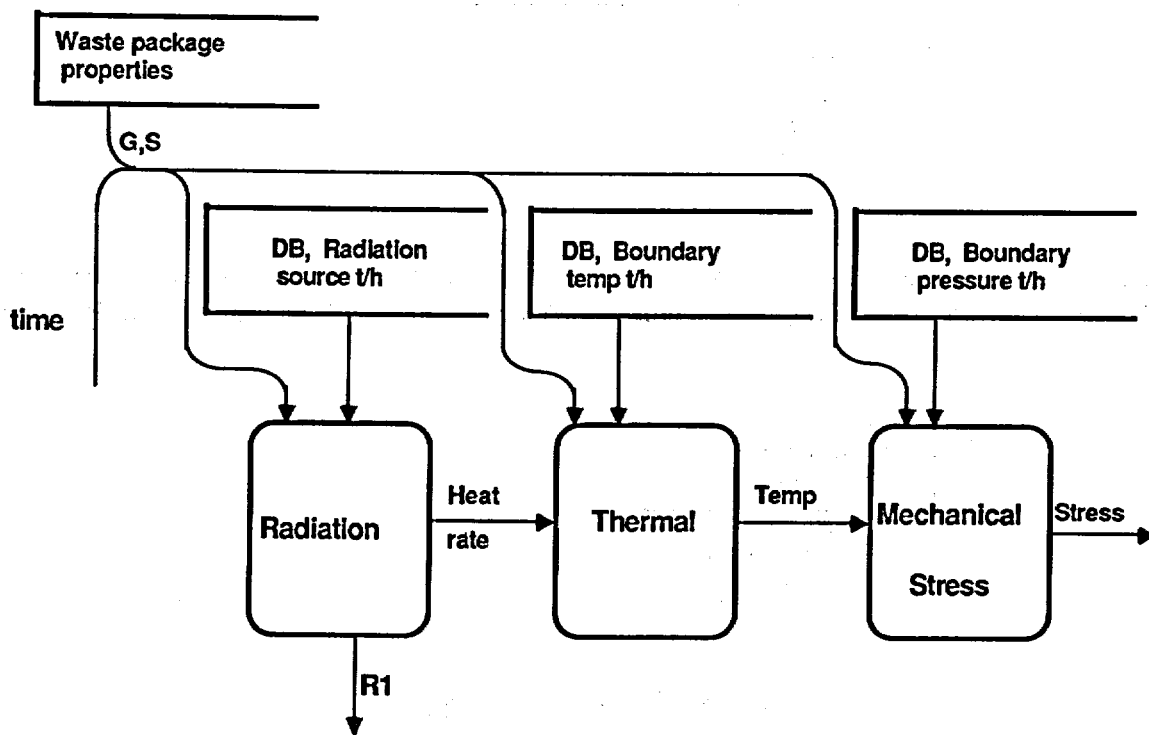


Figure 3-9. Data flows for the radiation, thermal, and mechanical stress processes. The process outputs shown—heat rate, temperature, and stress—adjust without time delay to the input boundary conditions. (Symbols and terms are defined in Table 3-5.)

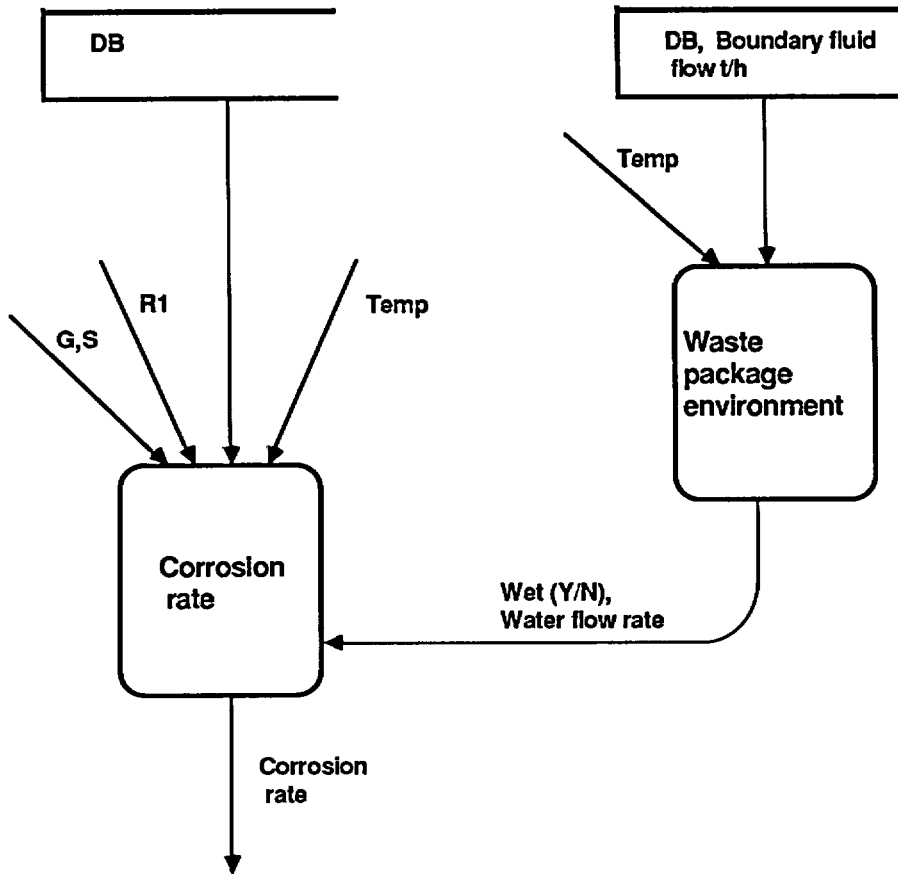


Figure 3-10. Data flows for the waste package environment and corrosion rate processes. The process outputs shown adjust without time delay to the input conditions. (Symbols and terms are defined in Tables 3-5 and 3-6.)

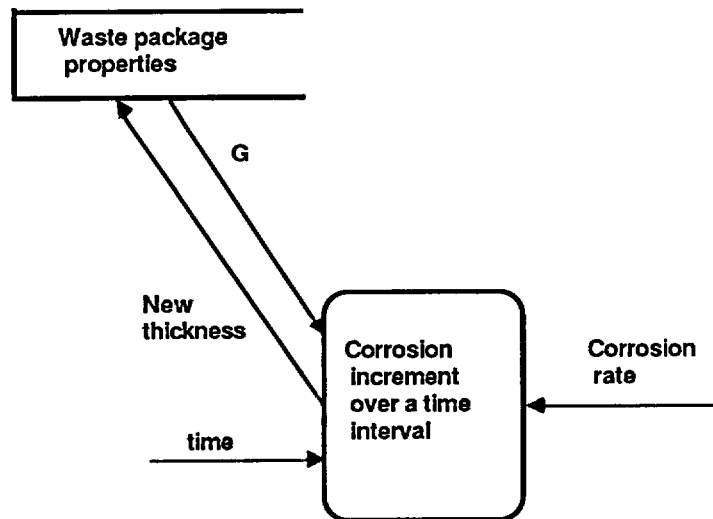
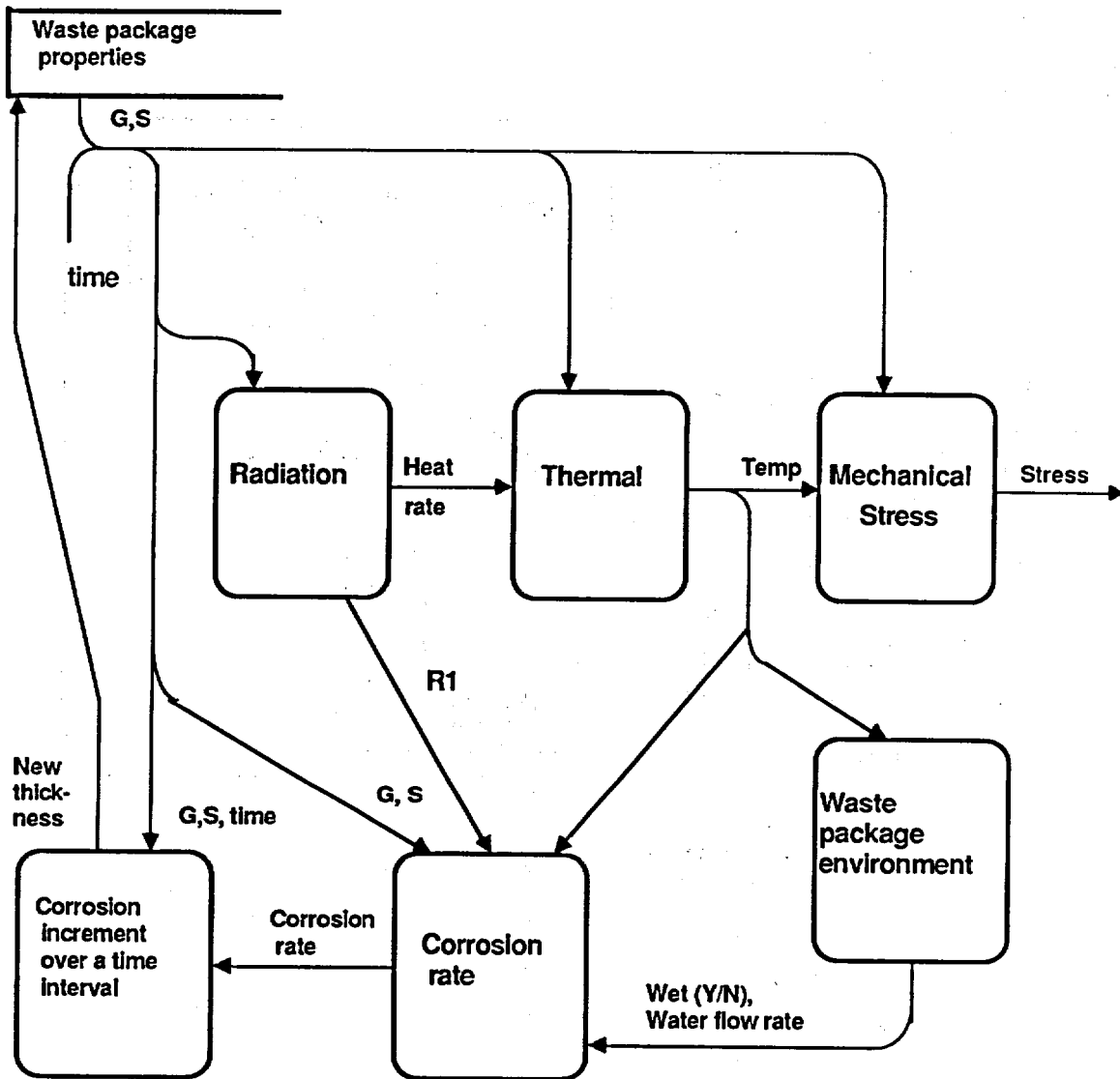


Figure 3-11. Data flows for the corrosion increment process. The output, new thickness, changes slowly; its value depends on past history as well as on current conditions. (Symbols and terms are defined in Tables 3-5 through 3-7.)

**Table 3-8. Data dictionary elements added for Fig. 3-13.**

Data label	Data contents
New barrier status, new dimensions, or no change	Any changes to waste package geometry or status
Time of loss of containment	Time of loss of containment function due to loss of barrier integrity



**Figure 3-12. Data flow diagram combining the processes shown in Figs. 3-9 through 3-11. Some of these processes are coupled in a continuous (over time) feedback loop. (Symbols and terms are defined in Tables 3-5 through 3-7.)**

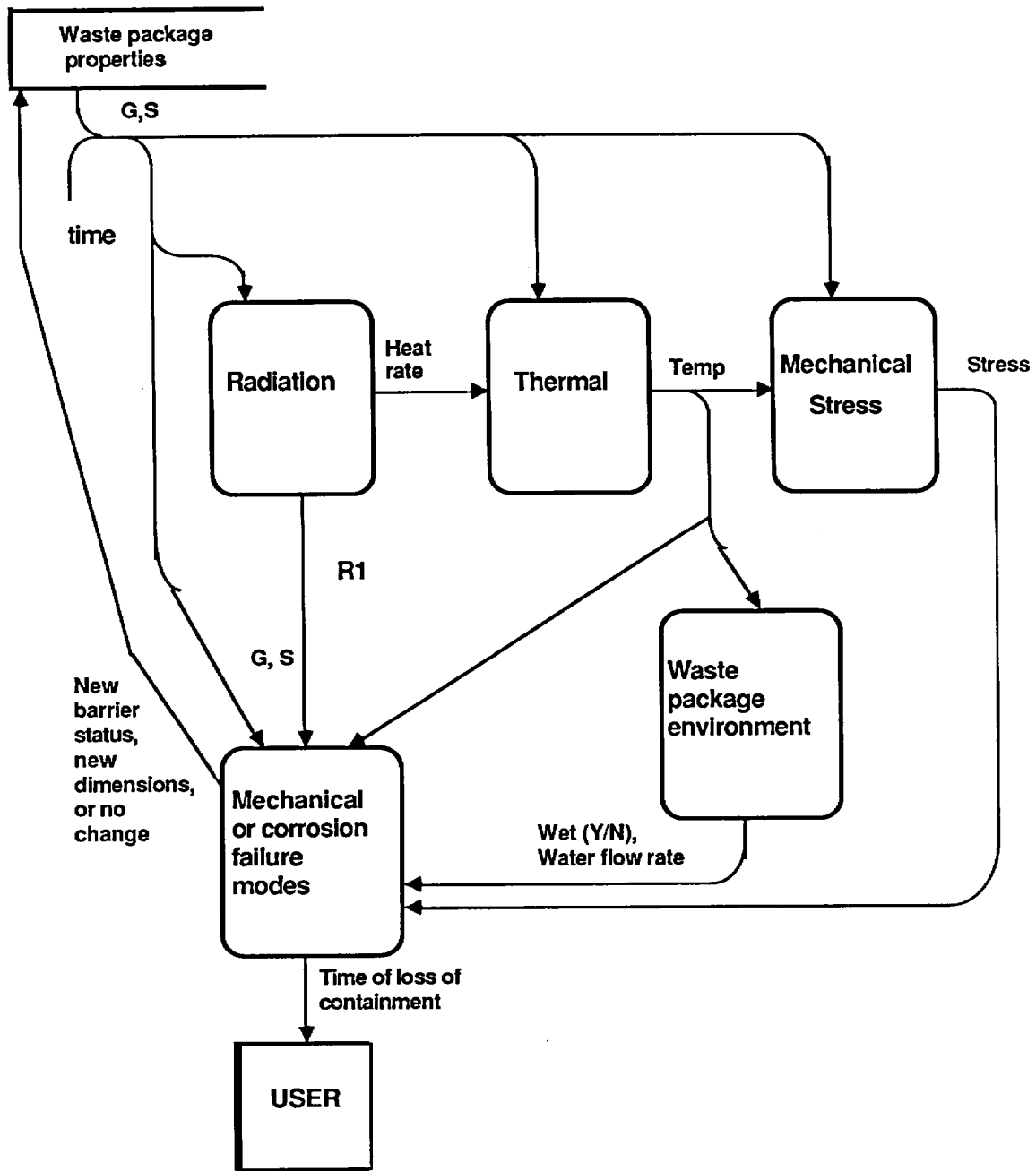
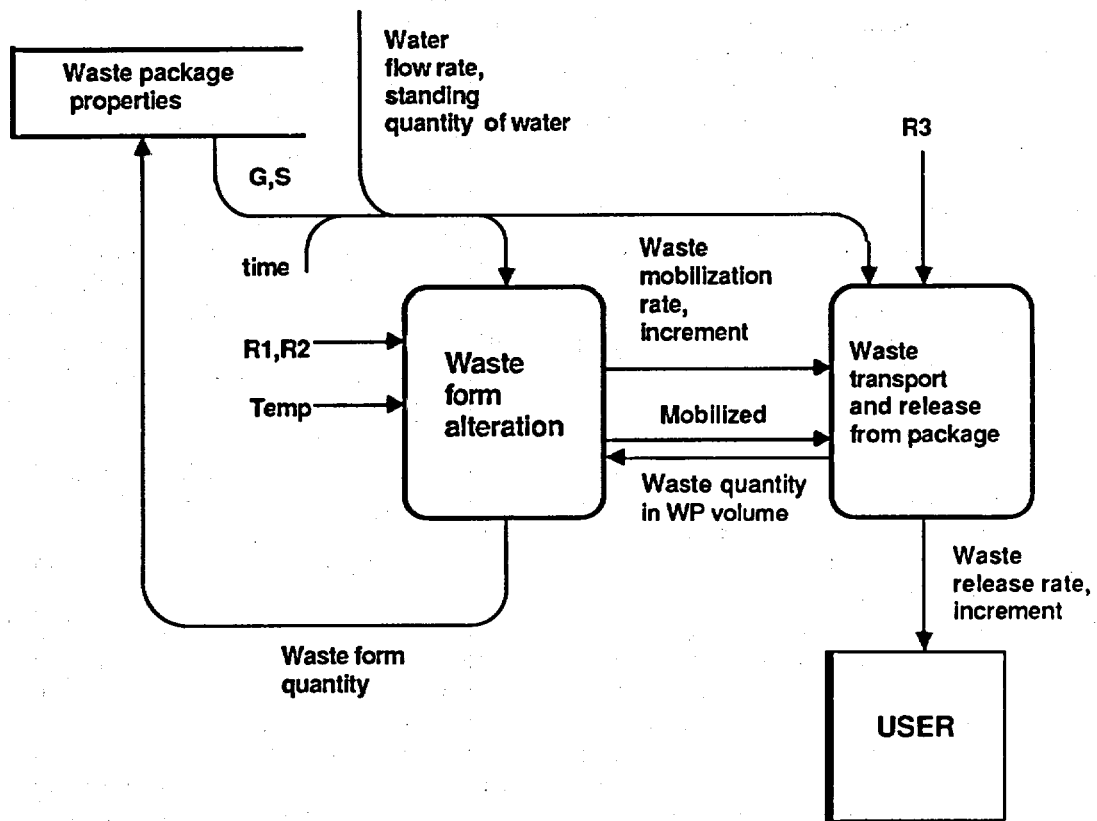


Figure 3-13. Data flow diagram showing the "mechanical or corrosion failure modes" process and the processes it depends upon for input data. There is a feedback loop present, but the feedback occurs only occasionally and by discrete amounts. (Symbols and terms are defined in Tables 3-5 through 3-8.)

**Table 3-9. Data dictionary elements added for Fig. 3-14.**

Data label	Data contents
R2	Radiation data: alpha particle dose (integrated up to current time) in waste form and alpha particle dose rate in water at waste form surface
R3	Radiation data: inventory of each radionuclide per unit of waste form
Standing quantity of water	Quantity of standing water in a partially degraded waste package
Waste mobilization rate, increment	Waste mobilization rate and increment of waste released from the waste form to the waste package volume during a time interval
Mobilized waste quantity in WP volume	Quantity of waste in mobile form and located within the waste package volume
Waste release rate, increment	Waste release rate and increment of waste released from the waste package to its exterior during a time interval



**Figure 3-14. Data flow diagram for the waste form alteration and waste transport processes. Inputs from other processes are shown by the data flow names. The outputs and some of the inputs change gradually and depend on past history as well as on current conditions. (Symbols and terms are defined in Tables 3-5 through 3-9.)**

## 4. Conclusions

We have developed the first generation of conceptual models for the long-term performance assessment of a nuclear waste package to be emplaced in a repository in an unsaturated tuff environment. The models of the processes and their interactions provide the specification for a first-generation computer program. The purposes of the first generation development are (1) to guide later generations of development and (2) to get first-approximation results examining interactions among the processes and evaluating proposed designs.

Our conceptual models use present knowledge and indicate an agenda for future information needs.

The radiation source model is a standard one and is implemented by data tables from a detailed model. Our gamma ray attenuation model is a new approximation of a well-understood but complex process. The goals of the approximation are simplicity and reasonably accurate results in variations or sensitivity analysis. We will need to do validation of this approximation.

Our thermal model uses steady-state heat transfer to determine the temperature field. Earlier studies using a time-varying heat transfer code have shown only small departures from the steady-state results.

The mechanical model uses well-understood principles for the elastic stress-strain range and somewhat conservative models for the limits of elasticity and for failure modes.

Future needs in the radiation, thermal, and mechanical areas include modeling of effects near the ends of the waste package, validating simplified models, and evaluating the achievable values in the simplification/accuracy trade-off.

The waste package environment excludes liquid water in early years after repository closure, when the local temperature is above the boiling point of water. The groundwater flow details near the waste package are presently unknown for the proposed emplacement geometry and the unsaturated, thermally changing conditions. We have a greatly simplified model which is conservative, possibly by orders of magnitude.

We include general corrosion in the first model, but defer localized corrosion modes such as pitting and stress corrosion cracking. It is unclear whether we can model these modes by establishing conservative bounds on go/no-go thresholds or whether we will need models including microscopic initiation and subcritical growth over the long time period of interest to waste package performance.

Waste form alteration and transport of waste to the waste package boundary are modeled by data tables to be developed from experiments. When the details of groundwater movement through a partially degraded waste package are developed, the corresponding responses of waste form alteration and waste transport processes may require more detailed models to describe the range of possible flow patterns and responses.

Our first generation computer code will be able to examine the interactions of processes affecting the waste package. Interactions among heat source, heat transfer, fluid flow, mechanical stress, and general corrosion are included in the first-generation model. Gamma radiation effects on corrosion can be included via data tables. The magnitudes of different radiation types -- gamma rays, alpha particles, spontaneous fissions, and neutrons -- will be calculated over time; their relative magnitudes can guide modeling of their effects in later generations of the model. The first-order effects of progressive degradation of barriers upon fluid flow will be calculated. The effects of fluid flow, temperature, and radiation upon waste form alteration and waste transport to the boundary of the waste package will be calculated.

Calculations with the first-generation computer code will quantify some (but not all) of the important consequences of design choices. Calculations will also indicate which processes and interactions modeled are most important. Calculations of magnitude of effects, sensitivity, and estimates of uncertainty or suspected bias (hopefully in a conservative direction) can identify present model simplifications most in need of refinement in the next generation model.

## References

1. P. J. Burns, *TACO2D—A Finite Element Heat Transfer Code*, Lawrence Livermore National Laboratory, Livermore, CA, UCID-17980, Rev. 2 (1982).
2. A. G. Croff, *A User's Manual for the ORIGEN2 Computer Code*, ORNL-TM-7175, Oak Ridge National Laboratory, Oak Ridge, TN (1979).
3. C. Gane and T. Sarson, *Structured Systems Analysis: Tools and Techniques* (Prentice-Hall, Inc., Englewood Cliffs, New Jersey, 1979).
4. J. N. Hockman and W. C. O'Neal, *Thermal Modeling of Nuclear Waste Package Designs for Disposal in Tuff*, Lawrence Livermore National Laboratory, Livermore, CA, UCRL-89820 Preprint (1984).
5. J. P. Holman, *Heat Transfer* (McGraw-Hill Book Company, New York, 1981), 5th ed.
6. J. H. Hubbell, "Photon Mass Attenuation and Energy-Absorption Coefficients from 1 keV to 20 MeV," *Int. J. Appl. Radiat. Isot.*, **33**, 1269 (1982).
7. INTERA Environmental Consultants, Inc., *WAPPA: A Waste Package Performance Assessment Code*, Battelle Memorial Institute, Office of Nuclear Waste Isolation, Columbus, OH, ONWI-452 (1983).
8. M. Jacob, *Heat Transfer* (John Wiley & Sons, Inc., New York), vol. I (1949), vol. II (1957).
9. A. Mendelson, *Plasticity: Theory and Application* (National Aeronautics and Space Administration, The MacMillan Company, New York, 1968).
10. P. Montazer and W. E. Wilson, *Conceptual Hydrologic Model of Flow in the Unsaturated Zone, Yucca Mountain, Nevada*, U.S. Geological Survey-Water Resources Investigations, Lakewood, CO, USGS-WRI-84-4345 (1984).
11. A. V. Nero, Jr., *A Guidebook to Nuclear Reactors* (Univ. of California Press, Berkeley, CA, 1979).
12. V. M. Oversby and C. N. Wilson, *Derivation of a Waste Package Source Term for NNWSI from the Results of Laboratory Experiments*, Lawrence Livermore National Laboratory, Livermore, CA, UCRL-92096 (1985).
13. K. Pruess and S. Y. Wang, *TOUGH—A Numerical Model for Nonisothermal Unsaturated Flow to Study Waste Canister Heating Effects*, Mat. Res. Soc. Symp. Proc., vol. 26, Elsevier Science Publishing Co., Inc. (1984).
14. T. Rockwell, III, *Reactor Shielding Design Manual* (D. Van Nostrand Company, Inc., Princeton, NJ, 1956).
15. W. Stein, J. N. Hockman, and W. C. O'Neal, *Thermal Analysis of NNWSI Conceptual Waste Package Designs*, Lawrence Livermore National Laboratory, Livermore, CA, UCID-20091 (1984).
16. R. T. Stula, T. E. Albert, B. E. Kirstein, and D. H. Lester, *Systems Study on Engineered Barriers: Barrier Performance Analysis*, prepared by Science Applications, Inc., for Office of Nuclear Waste Isolation, Battelle Memorial Institute, Columbus, OH, ONWI-211 (1980).
17. R. A. Van Konynenburg, *Radiation Doses in Granite Around Emplacement Holes in the Spent Fuel Test—Climax (Final Report)*, Lawrence Livermore National Laboratory, Livermore, CA, UCRL-53580 (1984).
18. R. A. Van Konynenburg, C. F. Smith, H. W. Culham, and C. H. Otto, Jr., *Behavior of Carbon-14 in Waste Packages for Spent Fuel in a Repository in Tuff*, Lawrence Livermore National Laboratory, Livermore, CA, UCRL-90855, Rev. 1 (1984).
19. C. Wang, *Applied Elasticity* (McGraw-Hill Book Company, New York, 1953).
20. T. P. Wilcox, R. A. Van Konynenburg, *Radiation Dose Calculations for Geologic Media Around Spent Fuel Emplacement Holes in the Climax Granite, Nevada Test Site*, Lawrence Livermore National Laboratory, Livermore, CA, UCRL-53159 (1981).
21. T. P. Wilcox, *MORSE-L, A Special Version of the MORSE Program Designed to Solve Neutron, Gamma, and Coupled Neutron-Gamma Penetration Problems*, Lawrence Livermore National Laboratory, Livermore, CA, UCID-16680 (1972).
22. Z. Zudans, T. C. Yen, and W. H. Steigelmann, *Thermal Stress Techniques in the Nuclear Industry* (The Franklin Institute Research Laboratories, Philadelphia, American Elsevier Publishing Company, Inc., New York, 1965).

## Appendix A. WAPPA's Gamma Ray Attenuation Model

Figure A-1 shows an output from WAPPA's gamma ray attenuation model. The plot shows the gamma ray flux at the surface of the waste form and the attenuated gamma ray flux at points outside the surface. The results were obtained by running a modification of a sample problem provided in the WAPPA report and code (INTERA, 1983). The modified problem kept the same waste form dimension and properties and modified some barrier dimensions.

The plotted results show two anomalies. First, the attenuated gamma ray flux immediately outside the surface is substantially higher than the flux at the surface before applying the attenuation model. Second, in annular air gaps the flux should drop off proportionally with  $1/\text{radius}$ , neglecting the small attenuation from the air mass present. (With cylindrical geometry, surface area increases linearly with radius.) The plotted results decrease more rapidly than  $1/\text{radius}$  in the air gap.

The two anomalies are probably due to the following conceptual error found in WAPPA. WAPPA adopted a model from the *Reactor Shielding Design Manual* (T. Rockwell III, Ed., 1956) but treated one variable in the model as a constant.

Rockwell's model (see Fig. A-2) involves two steps to calculate the gamma ray flux at a location P:

1. Find the attenuated flux of primary gamma rays. First, graphical correlations provided with the reference allow the solid source to be equated to a line source at a depth  $Z$  in the solid.  $Z$  is defined as the depth such that the attenuation of the primary gamma ray flux from the equivalent line source to the point of observation is the same as the average attenuation from the solid source. The attenuated primary flux from a line source is evaluated by a one-dimensional integration.

2. Calculate the total gamma ray flux by multiplying the primary gamma ray flux by a buildup factor. Because some secondary rays are created by Compton scattering of primary gamma rays, the total flux does not decrease as rapidly as does the primary flux. The ratio of the total flux to the primary flux is called the buildup factor.

$Z$  depends on (1) the radial distance  $a$  from the surface to the point of observation and (2) the shielding material in that distance; however, WAPPA treats  $Z$  as a constant. BARRIER (Stula et al., 1980) has the same model and the same error.

The buildup factor poses a potential data availability problem. The buildup factor depends primarily on the amount of absorbing material between

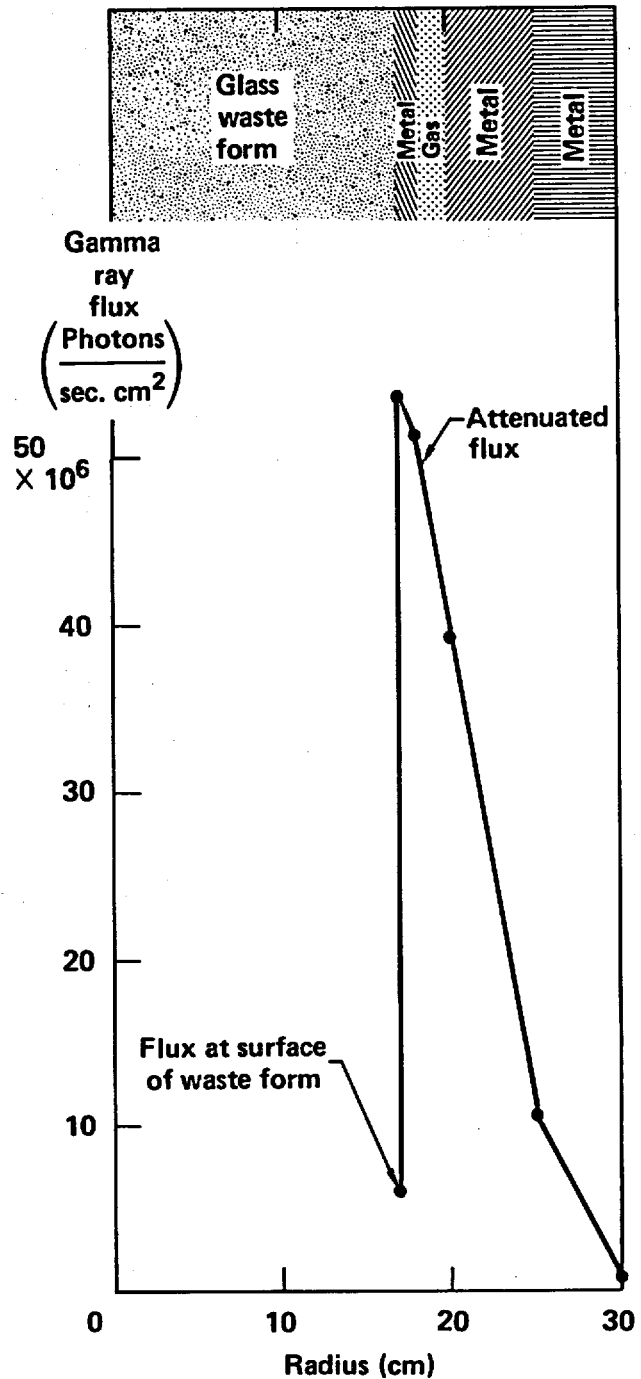


Figure A-1. Output from WAPPA's gamma ray attenuation model.

the source and the point of observation; it also depends on the geometry of placement of this material and on any material beyond the point of observation. Buildup factors have been published for some plane geometries but not for the geometries of the waste package and its exterior points of interest.

Because of the dependence of  $Z$  on distance and shielding (evaluated by a table look-up) and the limited data on buildup factors, a fresh evaluation of gamma ray attenuation is needed.

WAPPA computes this attenuated gamma ray flux but does not use it. As an input to barrier corrosion calculations WAPPA uses the unattenuated gamma ray flux from the waste form surface. This step avoids the problem in the attenuation model and provides a gamma ray flux value which is certainly greater than or equal to the true value. It removes the capability, however, to perform sensitivity analysis on the attenuation process and parameters.

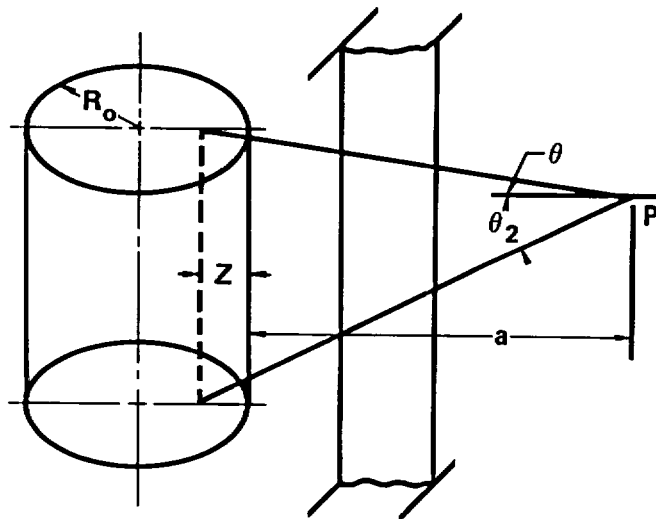


Figure A-2. Geometry for Rockwell's attenuation model from the *Reactor Shielding Design Manual*.

## Appendix B. PANDORA's Gamma Ray Dose Model

This appendix expands the discussion in Sec. 3.2.2.

The waste form is both a source and an attenuator of gamma rays. The metal barriers are attenuators of gamma rays. When water is present at the surface of a barrier or waste form, we want to compute the gamma ray absorbed dose rate in water because this causes radiolysis in the water which, in turn, may cause enhanced corrosion or enhanced alteration of the surface of the waste form.

The attenuation and the absorbed dose rate from gamma rays are complex processes. In a thick source, many of the gamma rays emerging from the surface are the result of scattering source gamma rays down to lower energies. For the source primary gamma rays of interest (about 0.4 MeV to 1 MeV), some of the gamma rays are absorbed by the photoelectric effect and some are shifted to lower energy (and altered direction) by Compton scattering. The lower energy (secondary) gamma rays are then subject to the same absorption and scattering processes. For light to medium elements (*i.e.*, oxygen to zirconium) and for primary gamma rays of interest here, Compton scattering dominates. Because of this scattering, the gamma ray flux emerging from the surface of the self-absorbing source has a spread of energies.

If there is a water layer on the surface of the source, some of the gamma ray energy flux can be absorbed in the water layer. The absorbed dose rate in the water layer depends on the energy distribution and the directional distribution of the gamma ray flux emerging from the source surface.

The required flux and absorbed dose parameters are not readily manageable by simple calculational methods. Therefore, we will take the results of a more complex calculation and scale them for the different source strengths and material layouts that may be selected for the nuclear waste packages.

The complex code we will use for our reference data is the MORSE-L Monte Carlo transport code (Wilcox, 1972). This code has a history of extensive use. Calculations for a spent fuel canister emplacement have been supported by measurements (Van Konynenburg, 1984).

The contribution of the new, simplified source model is that one reference simulation calculation, together with scaling and look-ups in the reference results, will serve for a range of similar waste forms and packaging geometries and for all times in the history of a waste package.

The mass energy-absorption coefficient  $\mu_{en}/\rho$  tells us what fraction of the primary gamma rays'

initial total energy has been transferred to kinetic energy of charged particles after traversal through a small thickness of material. The remaining fraction of the initial energy is transported further by secondary gamma rays and remaining primary gamma rays. (The thickness of material is measured in mass along the gamma ray's direction: density times length equals the mass per unit area perpendicular to this direction. Using this mass instead of length, the word "mass" appears in the name of the coefficient.) We can compare the attenuating effect of different atomic materials by comparing their coefficients  $\mu_{en}/\rho$ . The gamma ray flux has a spread of energies, but since the mass energy-absorption coefficient (see Fig. B-1) is nearly independent of gamma ray energy (over the range 0.4-1.0 MeV), then the fraction of energy taken out from each energy interval is about the same; therefore, the fraction of energy taken out from the whole flux is that same fraction. Hence, in comparing the attenuating effect on the gamma ray energy flux for different atomic materials, a comparison of their coefficients  $\mu_{en}/\rho$  at one typical gamma ray energy is a good first approximation for the comparison of overall effect. (The photoelectric absorption at the lower-end interval of the energy range makes a small modification to this result, which we neglect.)

For a uniform mass density, we can use  $\mu_{en}$  to quantify the energy absorption per unit length. The characteristic length  $L_{en}$  for gamma ray energy absorption is  $L_{en} = 1/\mu_{en}$ . We find that a single spent fuel rod is then (diameter is less than  $L_{en}$ ) allowing a simplified modeling of the spent fuel internal geometry. In a full waste package, whether of spent fuel or glass-based waste, the total waste form is thick (radius substantially greater than  $L_{en}$ ) allowing a simplified gamma ray source model.

In a spent fuel  $UO_2$  pellet,  $L_{en}$  is approximately 1.3 cm. The diameters of fuel pellets range up to 1.2 cm. Thus, a single fuel rod is thin. For gamma ray absorption, we may consider the spent fuel and Zircaloy cladding as a blended material. (The gas gaps between fuel rods do not contribute any appreciable amount to the absorption.) A package of fuel rods is much thicker than the gamma ray characteristic length  $L_{en}$ . For an annular packing with inner and outer radii of 15 cm and 30 cm, and packing to 50% solid  $UO_2$  in the volume (an underestimate), the annular thickness represents 5.7 times the effective  $L_{en}$  of the averaged material in that volume. For a single  $15 \times 15$  PWR fuel bundle (Van Konynenburg, 1981), the volume packing is 31%. The half thickness (10.7 cm) of the

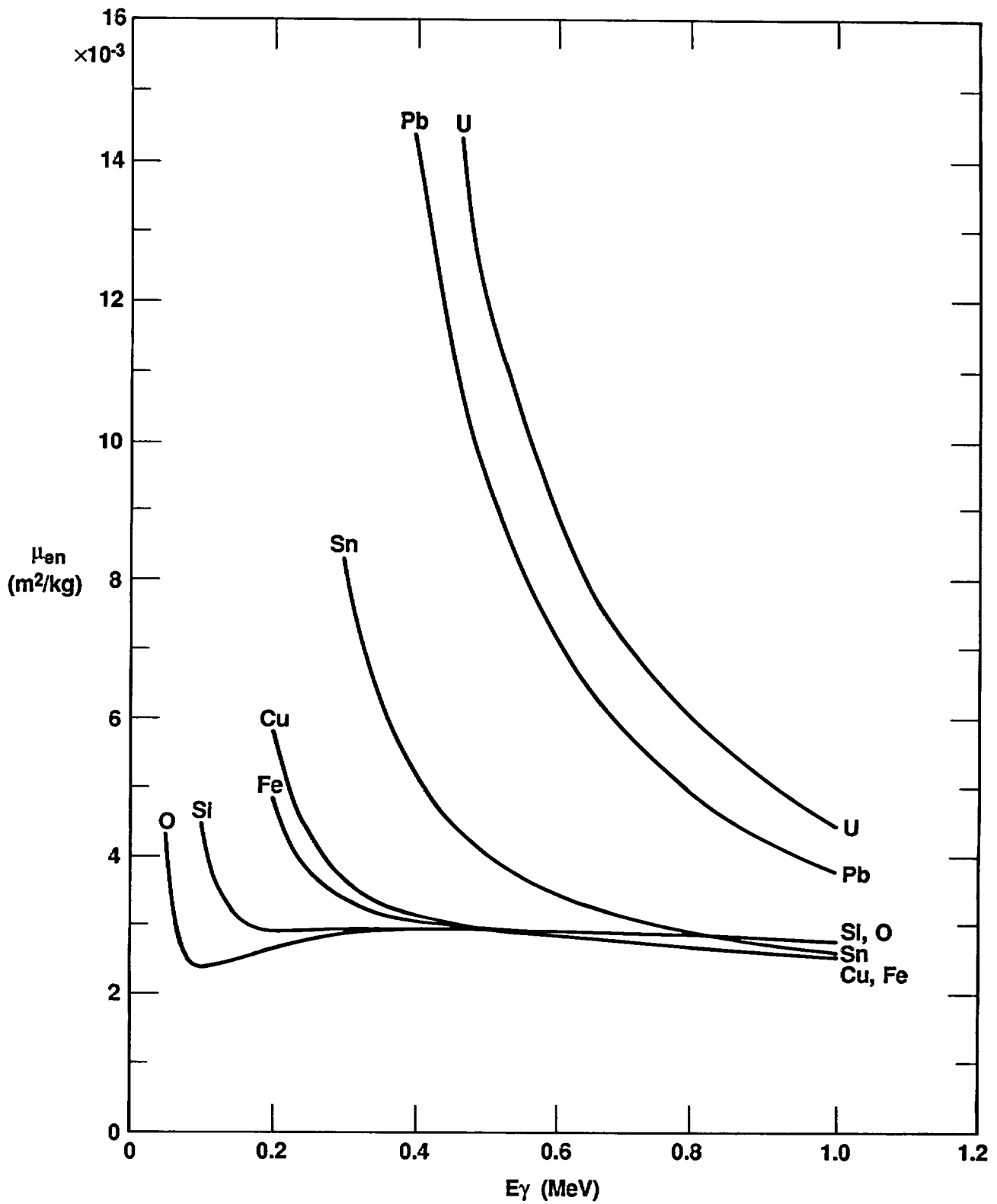


Figure B-1. Mass energy absorption coefficient ( $\mu_{en}/\rho$ ) for gamma rays.

bundle is 2.5 times the effective  $L_{en}$  of the averaged material.

In pure borosilicate glass,  $L_{en}$  is approximately 13 cm for a 0.7 MeV gamma ray. In defense waste with some nuclear waste elements and some inert elements (such as iron),  $L_{en}$  is somewhat smaller. With a radius  $r_o$  of 29.5 cm (see Fig. B-2),  $r_o/L_{en}$  is greater than 2.3.

The assumption of large  $r_o/L_{en}$  is used in the following development of a model for scaling of dose rate at the surface of the waste form.

The gamma ray mass energy absorption coefficients  $\mu_{en}/\rho$  are plotted in Fig. B-1. Between 0.4 and 1.0 MeV, the main constituents of glass (such as  $SiO_2$ ) and of metal barriers (such as iron and copper) have nearly equal and nearly constant  $\mu_{en}/\rho$ . Fission products have higher  $\mu_{en}/\rho$ . Tin (Sn) is plotted to indicate this; tin is intermediate between the two mass peaks in the fission product mass distribution. Uranium has a yet higher  $\mu_{en}/\rho$ .

For a reference waste form, the reference calculation gives the gamma ray absorbed dose rate in water at the surface of the waste form annulus.

The model's scaling of the gamma ray absorbed dose rate to a different waste form or to a different time in a waste form's history is:

1. Linear with the source gamma ray energy generation rate counting gamma rays above a threshold energy (to be determined, but perhaps 0.2 MeV for glass waste forms and 0.3 MeV for spent fuel);
2. Inverse with the mass density;
3. Multiplied by a weighting factor for changes in percentages of atomic composition of the waste form (in a future program version); and
4. Not dependent on the outer radius or inner radius.

The linear dependence on source energy generation rate was discussed in Sec. 3.2.2.1.

The inverse dependence on mass density is as follows. As mass density decreases, the characteristic energy-absorption length  $L_{en}$  increases:

$$\frac{1}{L_{en}} = \mu_{en} = \left( \frac{\mu_{en}}{\rho} \right) \cdot \rho . \quad (B-1)$$

The term  $(\mu_{en}/\rho)$  is a constant if the atomic composition (percentages by mass of the atomic constituents of the waste form) is unchanged, and will change by a small fraction if the atomic composition changes (see Eq. B-2 and discussion following Eq. B-2). The term  $\rho$ , the mass density, gives the inverse linear dependence of  $L_{en}$  on  $\rho$ . We next discuss the connection between  $L_{en}$  and the gamma ray energy flux and dose rate at the source surface, for a thick source.

As  $L_{en}$  increases, the number of source gamma rays within a depth  $L_{en}$  of the surface increases almost linearly with  $L_{en}$ . Source gamma rays from a fixed depth in the source are attenuated by the source's mass between that depth and the surface (see Fig. B-2). The contribution of source regions to flux at the surface decreases approximately exponentially with depth. There is a depth  $L''$  defined by the following: half of the gamma ray energy exiting the waste form surface originates from the zone within a depth  $L''$  from the surface.  $L''$  is less than  $L_{en}$  and is approximately in linear proportion to  $L_{en}$ ; the correspondence of  $L''$  to  $L_{en}$  becomes closer to linear as  $r_o/L_{en}$  becomes larger. (Recall that the waste forms have fairly large  $r_o/L_{en}$ ). In summary, mass density  $\rho$  affects  $L_{en}$  and  $L''$  and thereby affects the effective source zone for the surface flux. In net effect, the source surface gamma ray energy flux has an inverse linear dependence on  $\rho$ . The absorbed dose rate in water at the surface has the same inverse linear dependence on  $\rho$ .

Note that the preceding argument for the dependence on mass density was for a fixed concentration of source gamma rays per unit volume in the source. The

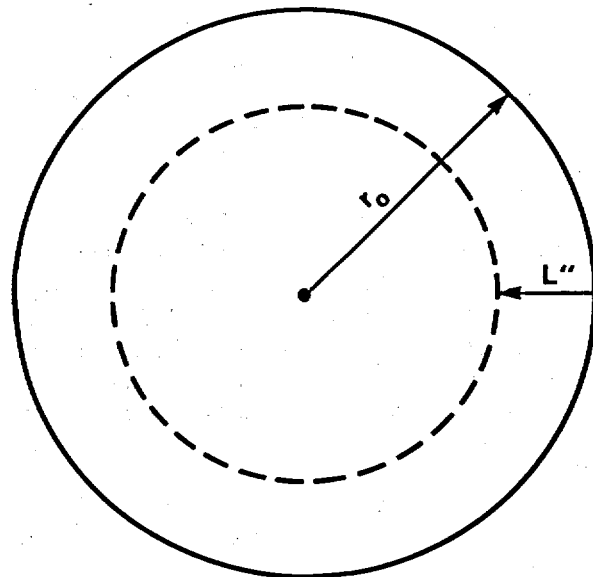


Figure B-2. Cross-sectional view of a cylindrical waste form with radius  $r_o$ . Most of the gamma ray energy originating in the deep interior is absorbed.  $L''$  is defined as follows. Half of the gamma ray energy exiting the waste form surface originates from the zone within a depth  $L''$  from the surface.  $L''$  is less than  $L_{en}$ .

source concentration was calculated by the radiation source model. If the source density and mass density are both increased (as in a closer packing of spent fuel rods of the same type), then the effects of both changes cancel, and the surface flux and the dose rate are unchanged. A thick source is the same source even if its packing density is changed.

The dependence of  $(\mu_{en}/\rho)$  on atomic number provides a secondary source of change in  $L_{en}$  and, hence, in source surface energy flux. In many cases this is only a small change that we can neglect. To be exact, we should use a weighted average  $(\mu_{en}/\rho)$ :

$$\left(\frac{\mu_{en}}{\rho}\right)_{\text{average}} = \frac{1}{\rho} \sum_i \left(\frac{\mu_{en}}{\rho}\right)_i \rho_i \quad (\text{B-2})$$

where the sum is over atomic elements  $i$ . This weighted average does not change by much, as shown by the following discussion. For a typical secondary gamma ray energy of 0.5 MeV (for elements from oxygen to copper), the  $(\mu_{en}/\rho)_i$  does not change by much. For a glass with tin (Sn) (to represent fission products) and lighter elements (O, Si, ...Fe), if the mass percentage of tin increases from 20% to 30%, the  $(\mu_{en}/\rho)_{\text{average}}$  increases by only 4.5%.

For spent fuel, uranium is predominant by mass and even more so by contribution to  $(\mu_{en}/\rho)_{\text{average}}$ . Spent fuels have varied design values in ratio of Zircaloy to uranium (depending mainly on fuel rod diameter) and varied amounts of burnup and, hence, percentages of fission products. But these make very little change in  $(\mu_{en}/\rho)_{\text{average}}$  because:

- The mass proportion of Zircaloy to  $\text{UO}_2$  changes by only a modest amount for different fuel designs. In one PWR fuel on a  $15 \times 15$  grid design (Nero, 1979), the Zircaloy constituted 25% of the volume occupied by solids and, thus, 18% of the mass and approximately 12% of the gamma ray attenuation in the composite solid. Variations in the Zircaloy fraction will cause variations in this 12% contribution to the attenuation.

- Similarly, variations from the typical 3% by mass of fission products will have only a very small effect on the attenuation in the fuel.

The insensitivity to radius  $r_o$  for gamma ray energy flux and absorbed dose rate in water at the waste form surface can be seen by reference to Fig. B-2. As  $r_o$  increases, the surface area increases linearly with  $r_o$ . Per unit area of surface, the number of source gamma rays within the depth  $L''$  of the surface hardly changes at all. (As an example, with  $r_o/L_{en} = 3$  and  $r_o/L'' = 8.6$ , if  $r_o$  increases by 10%, then the number of gamma rays within  $L''$  of the surface increases by only 0.5% per unit area of surface.)

In Sec. 3.2.2.2 we discuss the attenuation of gamma ray energy flux and of absorbed dose in water (if assumed present outside a barrier) by materials outside the waste form.

The gamma ray dose model has some limitations in accuracy compared to the full situation because of the simplifying approximations we use:

1. Mass energy absorption coefficients for materials across a range of atomic numbers are not quite equal.

2. The sources are thick (large  $r_o/L_{en}$  but not infinitely thick; a small effect of radius was noted two paragraphs above.

3. Some waste form shapes are only coarsely approximated by a cylinder (see especially Figs. 2-1 and 2-3).

4. Spent fuel in the form of fuel assemblies could have some streaming effect in the open channels between rows of fuel rods; i.e., gamma rays once scattered into a channel can travel further before scattering, and some near-forward scattering will keep some of these gamma rays moving within the channel. The net result is more gamma rays exiting from the channels; i.e., a spatial variation on the average gamma ray flux from our space-averaged source model.

All of these limitations allow simplification of the model while the major factors influencing outcome are modeled. The effect of these limitations on accuracy should be quantified in future work.

*Technical Information Department* • Lawrence Livermore National Laboratory  
University of California • Livermore, California 94550

